CHAPTER 4

Spin Waves Above the Threshold of Parametric Excitations

V.S. L'VOV

Institute of Automation and Electrometry
Siberian Branch of the USSR Academy of Sciences
630090 Novosibirsk, USSR

and

L.A. PROZOROVA

Institute for Physical Problems
USSR Academy of Sciences
117334 Moscow, USSR

Translated from the Russian by Nicholas Weinstein

Contents

List of symbols

a_k	amplitude of spin wave with wavevector $\boldsymbol{k}$
A	hyperfine interaction constant
C	$=\eta/\lvert S\rvert$
C_3, C_6	crystallographic axes
CO	collective oscillations
d	dimension of the sample
g	magnetomechanical factor
$\boldsymbol{h}$	microwave magnetic field
h_{th}	threshold field for parametric excitation of SW
$\boldsymbol{H}$	static magnetic field
H_A	anisotropy field
H_D	Dzyaloshinsky field
H_E	exchange field
H_Δ	gap in the SW spectrum for $H = 0$
$\mathscr{H}$	Hamiltonian
I	nuclear spin
$I(\omega)$	spectral composition of radiation
$\boldsymbol{k}$	wavevector of SW in units of cm^{-1}
m_z	longitidunal components of the magnetization
M	magnetization
$n(\boldsymbol{k})$	normal correlation function
N	number of PSW
N_T	number of thermal SW
N_z	demagnetization factor
PSW	parametrically excited SW
$S_{kk'}$	coefficient of the Hamiltonian
SW	spin wave
T	temperature
$T_{kk'}$	coefficient of the Hamiltonian
T_C	Curie temperature
T_N	Néel temperature
v_s	velocity of sound
$v(\boldsymbol{k})$	group velocity of SW
V	coefficient of the magnon–pump field coupling
W_+	absorbed power
W_-	dissipated power
α_i	inhomogeneous exchange constant
β	$=\eta N_T/kv$
γ	damping of SW
Δ	frequency shift
$\Delta\omega$	PSW packet width
η	nonlinear damping factor
ϑ	polar angle
θ	magnetoelastic interaction constant
λ	SW length
μ_B	Bohr magneton
ξ	supercriticality, h/h_{th}
$\sigma(\boldsymbol{k})$	anomalous correlation function
τ	magnon life time
φ	azimuthal angle
$\varphi(\boldsymbol{k})$	phase of SW
χ	high-frequency susceptibility, $\chi' + i\chi''$
Ψ	phase of a pair of SW
Ψ_p	pump phase
ω	SW frequency
ω_p	pump frequency
ω_{ex}	exchange frequency
Ω	frequency of CO
$\boldsymbol{\Omega}$	direction of wavevector of SW, $\boldsymbol{k}/k$

1. Introduction

The nonlinear dynamics and kinetics of magnetically ordered dielectrics—ferro- and antiferromagnets—are being intensively developed at present. This branch of physics deals with the behavior of magnetic systems under the powerful external action of an electromagnetic microwave field, laser radiation, ultrasound, etc. Under these conditions, quasiparticles (magnons, phonons, etc.) are strongly excited, and the nonlinear behavior of the magnetic system depends to a considerable extent on the interactions of the quasiparticles. Most widely investigated is the parametric excitation of spin waves by microwave pumping.

The present review deals with experimental and theoretical investigations of nonlinear effects in the parametric excitation of spin waves (SW) in ferro- and antiferromagnets. The problem of the parametric resonance of SW arose in the fifties, in connection with the research of Bloembergen and Damon (1952) and Bloembergen and Wang (1954) on ferromagnetic resonance at high power levels. They discovered "additional" absorption of energy of the uniform precession of the magnetization with a sharply defined threshold in the intensity of the microwave pumping.

Suhl (1957) explained this phenomenon as the parametric decay of uniform precession into a SW pair. In 1960, Morgenthaler (1960) and, independently, Schlömann, Green and Milano (1960) predicted (and the last three discovered, in YIG) the phenomenon of "parallel pumping": the parametric excitation of SW by a microwave magnetic field $\boldsymbol{h}(t)$ with polarization $\boldsymbol{h} \| \boldsymbol{H}$ (where $\boldsymbol{H}$ is the static magnetic field). This phenomenon occurs if the amplitude of h exceeds a threshold value h_{th}, which is determined by the SW damping. It can be interpreted as the decay of a single photon into two magnons, satisfying the conservation law

$$\hbar\omega_{\text{p}} = \hbar\omega(\boldsymbol{k}_1) + \hbar\omega(\boldsymbol{k}_2), \quad 0 = \boldsymbol{k}_{\text{p}} = \boldsymbol{k}_1 + \boldsymbol{k}_2. \tag{1}$$

In the following years, parallel pumping became one of the principal methods of generating SW in magnetic systems. The phenomenon of parallel pumping of SW in antiferromagnets (AFM) was discovered in 1969 independently by Seavey (1969a) and by Prozorova and Borovik-Romanov (1969).

The first models to describe the limitation of the amplitude of parametric

SW (PSW) were proposed in the sixties. An important step along this line was the work of Suhl (1957), who showed that in the excitation of SW by uniform precession of the magnetization, the principal limiting mechanism is the reverse effect of PSW on pumping, leading to "freezing" of the precession amplitude at the threshold level. But attempts to explain the experimentally observed phenomenon with parallel pumping encountered considerable difficulties. The application of methods to limit the parametric instability, traditional for parametric resonance in systems with a small number of degrees of freedom, such as nonlinear damping and nonlinear frequency detuning, showed the inadequacy of these methods. In many cases, the nonlinear damping was too weak to be able to explain the observed SW level. Nonlinear frequency detuning does not limit parametric resonance at all in a medium with a continuous wave spectrum, because there are always waves whose renormalized frequencies exactly satisfy the resonance conditions. An important step forward was made by Schlömann (1959), who drew attention to the necessity to take into account the nonlinear interaction of PSW with one another, and suggested that the main contribution to this interaction is made by four-magnon processes with the conservation laws

$$\omega(\boldsymbol{k}) + \omega(-\boldsymbol{k}) = \omega(\boldsymbol{k}') + \omega(-\boldsymbol{k}'). \tag{2}$$

A new period in the investigation of nonlinear phenomena in the parametric excitation of waves began in 1969–70 with the research of Zakharov, L'vov and Starobinets (1969, 1970). These authors showed that processes of the type of eq. (2) weaken the coupling of the SW with the pump field and, as a result, limit their amplitude. Such a "phase" mechanism for the limitation of the amplitude of waves was found to be essential in parallel pumping. Processes of the type of eq. (2) can be conveniently studied after diagonalization of the Hamiltonian of wave interaction, similar to the BCS approximation in superconductivity theory. The theory proposed by Zakharov, L'vov and Starobinets based on this approximation, was subsequently called the *S*-theory (Zakharov et al. 1970). In investigations conducted in 1970–74, these three physicists and their colleagues succeeded in making considerable progress within the framework of the *S*-theory and its generalizations. Their progress consisted in a detailed study of the properties of PSW, in a qualitative explanation of many effects observed in experiments and in the achievement of satisfactory quantitative agreement with experimental data (Zautkin et al. 1970, L'vov and Starobinets 1971, Zautkin et al. 1972a,b, Zakharov et al. 1972, 1974). Clarified, among other matters, within the scope of the *S*-theory were the gigantic self-oscillations of the magnetization in the parametric excitation of SW. These oscillations were first observed in 1961 by Hartwick, Peressini and Weiss (1961) and were subsequently investigated experimentally in detail.

Research conducted by G. Melkov, L. Prozorova, V. Ozhogin, V. Zautkin and their coworkers yielded interesting and important results associated with a

new understanding of the physical meaning of the phenomena occurring above the threshold of parametric excitation of waves. The basic conclusions of the *S*-theory were confirmed, details of the nonlinear behavior of SW were clarified, and qualitatively new nonlinear effects were discovered. These effects were difficult to predict theoretically.

2. *Parametric instability of spin waves in magnetic dielectrics*

2.1. *Equations of motion*

Employing the procedure of Zakharov et al. (1970), we select the equations of motion in the quasi-Hamiltonian form:

$$\mathrm{i}[\mathrm{d}a_k/\mathrm{d}t + \gamma(\boldsymbol{k})a_k] = -\delta\mathscr{H}/\delta a_k. \tag{3}$$

Here a_k is the amplitude of a propagating SW with wavevector $\boldsymbol{k}$:

$$a(\boldsymbol{r}, t) = a_k \exp\{\mathrm{i}[\boldsymbol{k}\cdot\boldsymbol{r} - \omega(\boldsymbol{k})t]\}, \tag{4}$$

while $\gamma(\boldsymbol{k})$ is the damping of PSW due to their interaction with thermal SW, phonons, etc. The Hamiltonian $\mathscr{H}$ is of the form

$$\mathscr{H} = \mathscr{H}_0 + \mathscr{H}_\mathrm{p} + \mathscr{H}_\mathrm{int}, \tag{5}$$

where $\mathscr{H}_0$ is the Hamiltonian of noninteracting SW:

$$\mathscr{H}_0 = \sum_{\boldsymbol{k}} \omega(\boldsymbol{k}) a_k a_k^*, \tag{6}$$

and $\mathscr{H}_\mathrm{p}$ describes the interaction of SW with the microwave pump field $h(t) = h\exp(-\mathrm{i}\omega_\mathrm{p}t)$. When $\boldsymbol{h}\|\boldsymbol{H}$ (Morgenthaler 1960, Schlömann et al. 1960),

$$\mathscr{H}_\mathrm{p} = \sum_{\boldsymbol{k}} \mathscr{H}_\mathrm{p}(\boldsymbol{k}), \quad \mathscr{H}_\mathrm{p}(\boldsymbol{k}) = \tfrac{1}{2}[hV_k \exp(-\mathrm{i}\omega_\mathrm{p}t)\, a_k a^*_{-k} + \mathrm{c.c.}]. \tag{7}$$

Making use of the fact that all PSW have nearby frequencies, we can retain in Hamiltonian $\mathscr{H}_\mathrm{int}$ only the terms that describe four-magnon processes,

$$\mathscr{H}_\mathrm{int} = \frac{1}{2}\sum_{1,2,3,4} T_{12,34} a_1^* a_2^* a_3 a_4\, \delta(\boldsymbol{k}_1 + \boldsymbol{k}_2 - \boldsymbol{k}_3 - \boldsymbol{k}_4). \tag{8}$$

Here $a_i = a_{k_i}$, and $T_{12,34} = T(\boldsymbol{k}_1\boldsymbol{k}_2, \boldsymbol{k}_3\boldsymbol{k}_4)$ is the total amplitude of four-magnon processes.

Equations (3) through (8) are the basic equations in the analysis of the behavior of SW above the threshold of parametric excitation.

2.2. *Threshold of parametric excitation of spin waves*

In order to calculate the threshold of parametric excitation of SW let us

consider the expression for the flux of energy $W_+(\boldsymbol{k})$ transferred from the pump field to a pair of waves $\pm\boldsymbol{k}$:

$$W_+(\boldsymbol{k}) = \partial\mathscr{H}_p(\boldsymbol{k})/\partial t = i\omega_p(hV_k b_k^* b_{-k}^* - \text{c.c.})$$
$$= 2\omega_p|hV_k||b_k|^2 \sin[\Psi_p(\boldsymbol{k}) - \Psi(\boldsymbol{k})]. \tag{9}$$

Here $b_k(t)$ are slow variables,

$$b_k(t) = a_k(t)\exp(\tfrac{1}{2}i\omega_p t), \quad b_k = |b_k|\exp[i\varphi(\boldsymbol{k})]; \tag{10}$$

$\Psi(\boldsymbol{k}) = \varphi(\boldsymbol{k}) + \varphi(-\boldsymbol{k})$ is the phase of the pair, and $\Psi_p(\boldsymbol{k}) = \arg(hV_k)$ is the phase of the pump field. The energy $W(\boldsymbol{k})$ dissipated per unit time by the pair is equal to

$$W_-(\boldsymbol{k}) = 2\gamma(\boldsymbol{k})\omega_p|b_k|^2. \tag{11}$$

Energy balance, $W_+ = W_-$, is valid for the threshold values. A maximum energy flux and a minimum instability threshold is obtained for pairs with the most favorable phase relation, $\Psi(\boldsymbol{k}) = \Psi_p(\boldsymbol{k}) + \pi/2$, for which the relation for the threshold is $|hV_k| = \gamma(\boldsymbol{k})$. The condition of parametric resonance can obviously be satisfied simultaneously by a large number of pairs whose wavevectors lie on the resonance surface, eq. (1). Pairs for which the ratio $\gamma(\boldsymbol{k})/|V_k|$ is minimal have the minimum excitation threshold,

$$h_{th} = \min[\gamma(\boldsymbol{k})/|V_k|]. \tag{12}$$

2.3. Experimental investigations of the parametric excitation of spin waves

2.3.1. Experimental procedure and investigated substances

As has been mentioned in the Introduction, the first experiments on the excitation of SW by "parallel pumping" were conducted quite some time ago (1960) on a yttrium iron garnet (YIG) crystal, which still remains one of the most popular objects used in this type of research. Today, parametric instability has been observed in a number of magnetic systems. These include, besides ferrites, low-dimensional ferro- and antiferromagnets, as well as three-dimensional antiferromagnets with various magnetic symmetries.

Research is carried out in the microwave range. Usually simple microwave spectrometers with direct amplification are used. The block diagram for one such setup is shown in fig. 1. The sample, oriented in a definite direction, is placed within the resonator at the antinode of a microwave magnetic field $\boldsymbol{h}\|\boldsymbol{H}$. The operating conditions of the microwave generator are selected in accordance with the specific aim of the investigations. Parametric excitation of SW is registered by the appearance of additional absorption at sufficiently high microwave power. If the generator is arranged for pulsed operation, it is possible to follow the development of the instability with time. The amplitude of the microwave magnetic field h in the sample is calculated from the

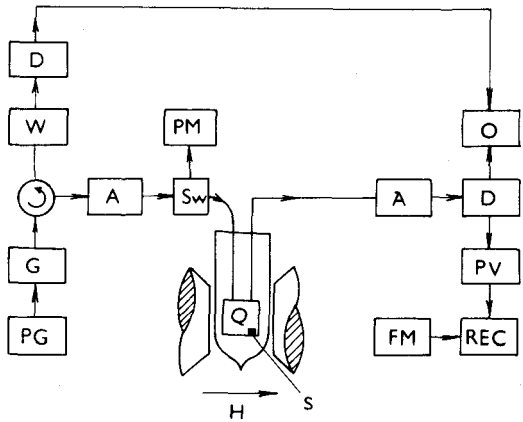

Fig. 1. Block diagram of the spectrometer for observing parametric excitation of SW: G, microwave generator; A, attenuator; D, crystal detector; Sw, switch; W, wavemeter; PM, power meter; Q, cavity resonator; PV, peak-value voltmeter; FM, field meter; REC, recorder; PG, pulse generator; O, oscilloscope; S, sample (Kotyuzhansky and Prozorova 1972).

magnitude of the microwave power in the resonator, and the resonator parameters. The threshold field h_{th}, above which parametric excitation appears, is directly related, by eq. (12), to the damping $\gamma(\boldsymbol{k})$ of the excited SW.

The calculation of $\gamma(\boldsymbol{k})$ from h_{th} is a traditional procedure in investigations of damping. Most of the research conducted on parallel pumping concerns such damping investigations and the clarification of the specific mechanisms for the interactions of SW with other excitations and with the inhomogeneities of the sample. The nature of the stationary state above the threshold of parametric excitation was investigated only in yttrium iron garnet samples and the easy-plane antiferromagnets $MnCO_3$, $CsMnF_3$ and $FeBO_3$. We will also concentrate our attention on the experimental investigations of these substances. First of all we shall discuss the spectrum $\omega(\boldsymbol{k})$ and damping $\gamma(\boldsymbol{k})$ of SW, because this is of special importance for what follows.

2.3.2. Spin wave spectra (theoretical data)

(a) *Yttrium iron garnet (YIG).* The cubic ferromagnet yttrium iron garnet, $Y_3Fe_5O_{12}$, has a complex crystalline structure. Its unit cell contains four formula units, with the magnetic Fe^{3+} ions occupying two nonequivalent positions of octahedral (a) and tetrahedral (d) symmetry. At $T < T_c = 560\,\text{K}$, YIG is a ferromagnet with collinear ordering. In the unit cell of YIG there are 20 magnetic ions (8a + 12d). Twenty magnon branches of the spectrum fall in the energy range from 0 to 1000 K. The frequencies of uniform oscillations were theoretically calculated by Douglass (1960) and approximate expressions for the frequencies $\omega_j(\boldsymbol{k})$ throughout the whole Brillouin zone were obtained

by Kolokolov et al. (1983). One branch of the spectrum $\omega_1(\boldsymbol{k}) \equiv \omega(\boldsymbol{k})$ is quasi-ferromagnetic and has no energy gap in the exchange approximation. For long SW

$$\omega(\boldsymbol{k}) = \omega_{ex}(a\boldsymbol{k})^2, \tag{13}$$

where ω_{ex} is the exchange frequency and a is the lattice constant ($\hbar\omega_{ex} = 40$ K and $a = 12.5$ Å). Taking the magnetic dipole interaction into account leads to a more complex expression for the long-wavelength part of the spectrum,

$$\omega^2(\boldsymbol{k}) = [\omega_i + \omega_{ex}(a\boldsymbol{k})^2 + \tfrac{1}{2}\omega_m \sin^2\vartheta][\omega_i + \omega_{ex}(a\boldsymbol{k})^2], \tag{14}$$

where $\omega_i = gH - \omega_m N_z$ and $\omega_m = 4\pi g M$. Here $\boldsymbol{M}$ is the magnetization, g is the magnetomechanical factor, N_z is the demagnetization factor and ϑ is the polar angle of SW propagation. ($4\pi M = 1730$ Oe at $T = 300$ K, $g = 2\pi \cdot 2.8$ GHz/kOe and $N_z = 1/3{,}1$ and 0 for a spherical sample, and for a magnetized thin disk, in the normal and tangent directions respectively.) For $k < 10^5\,\mathrm{cm}^{-1}$, $\omega(\boldsymbol{k})$ falls in the microwave range. The other branches of the spectrum have frequencies above 1000 GHz and were experimentally investigated only by means of neutrons (Plant 1977).

(b) *Antiferromagnets with "easy-plane" anisotropy.* To this class belong uniaxial antiferromagnets (AFM) (with a high-order C_3 or C_6 axis) in which the ion magnetic moments lie in the basal plane. The anisotropy in this plane is negligibly small. The two-sublattice model is usually used to describe the properties of such AFM. For $H = 0$ the moments of the sublattices may be either anti-parallel ($CsMnF_3$) or, if so allowed by symmetry, weakly canted ($MnCO_3$ and $FeBO_3$). In the latter case, the substance possesses a spontaneous magnetic moment, i.e,. it is a "weak ferromagnet". To describe this property in a phenomenological theory use is made of the Dzyaloshinsky field H_D (Dzyaloshinsky 1957). In the two-sublattice model the SW spectrum of these AFM consists of two branches ($\boldsymbol{H} \perp C_3$ or $\boldsymbol{H} \perp C_6$) (Borovik-Romanov 1958, Turov 1959):

$$\omega_1^2(\boldsymbol{k}) = g^2[H(H + H_D) + H_\Delta^2 + (\alpha_i k_i)^2], \tag{15}$$

$$\omega_2^2(\boldsymbol{k}) = g^2[2H_A H_E + H_D(H + H_D) + (\alpha_i k_i)^2], \tag{16}$$

where H_A and H_E are the anisotropy and exchange fields, respectively, H_Δ^2 is a term determined by various weak interactions, and α_1 are the inhomogeneous exchange constants (in the cubic approximation $g\alpha_i = \omega_{ex} a$). SW belonging to the low-frequency branch of the SW spectrum are parametrically excited. The relation $\omega_1(\boldsymbol{k})$ for this branch differs from $\omega(\boldsymbol{k})$ [see eq. (13)] for a ferromagnet (YIG): it is quasi-linear (rather than quadratic), i.e., far from the gap

$$\omega_1(\boldsymbol{k}) = g\alpha_i k_i, \tag{17}$$

and the dipole broadening of the spectrum is very small.

2.3.3. Spin wave spectra (experimental data)

There exist numerous experimental methods to determine the constants of the SW spectrum. Electron magnetic resonance (either ferromagnetic or antiferromagnetic) is usually resorted to determine the "spectral gap," i.e. the frequency of uniform oscillations. This method assures maximum accuracy. The inhomogeneous exchange constants can be obtained from the temperature dependences of the specific heat and the magnetization, data on inelastic neutron scattering, two-magnon scattering of light, etc. We shall discuss two kinds of experiment in which these constants are determined by using the parametric excitation of SW by parallel pumping.

(a) *Size effect.* This effect was discovered by Jantz and Schneider on monocrystalline spheres of YIG (Jantz et al. 1972), and then observed by Kotyuzhansky and Prozorova (1980) on plates of $FeBO_3$. This effect is as following: At low SW damping, when the free path length of the SW is larger than the dimensions of the sample, the power passing through the resonator is not a monotonic function of H, but has dips of a resonance type at definite values H_n. It is natural to explain the observed phenomenon by the effect of the boundary conditions on the surface of the sample leading to SW resonance, at

$$n\lambda = 2d. \tag{18}$$

Here d is the dimension of the sample, $\lambda = 2\pi/k$ is the SW length and n is an integer. (As a rule in these experiments $d \approx 0.1$ cm, and $k = 10^4$ to 10^5 cm^{-1}, and, consequently, $n \approx 10^3$.) The validity of such an explanation was checked experimentally, using samples of various sizes. The results of one such experiment are shown in fig. 2. The distance ΔH between the dips can be calculated from condition (18) and equations describing the SW spectrum. From a comparison of the experimental and theoretical values of ΔH the frequencies ω_{ex} and ω_1 can be calculated.

(b) *Threshold anomaly in the region of the intersection of the spin wave and phonon spectra.* The magnon and phonon branches of the energy spectra can have points of intersection. If the symmetry of the crystal allows interaction between these branches, the spectra will be distorted in the vicinity of these intersections. "Mixed" magnetoelastic oscillations exist in these regions and their damping differs from SW damping. Therefore h_{th} can change appreciably near such points of intersection. This phenomenon was first observed by Turner (1960) on YIG monocrystals. Subsequently, this effect was studied on easy-plane antiferromagnets (among others in $CsMnF_3$ and $MnCO_3$) (Seavey 1969b, Kveder et al. 1972, Kotyuzhansky and Prozorova 1971, 1973), in spectra which had points of intersection at nonzero field. Such anomalies in $CsMnF_3$ are shown in fig. 3a; they are seen as peak-like changes in the energy absorbed by the sample when the points of intersection of the spectra are passed by varying the field H. The experiments were conducted with various

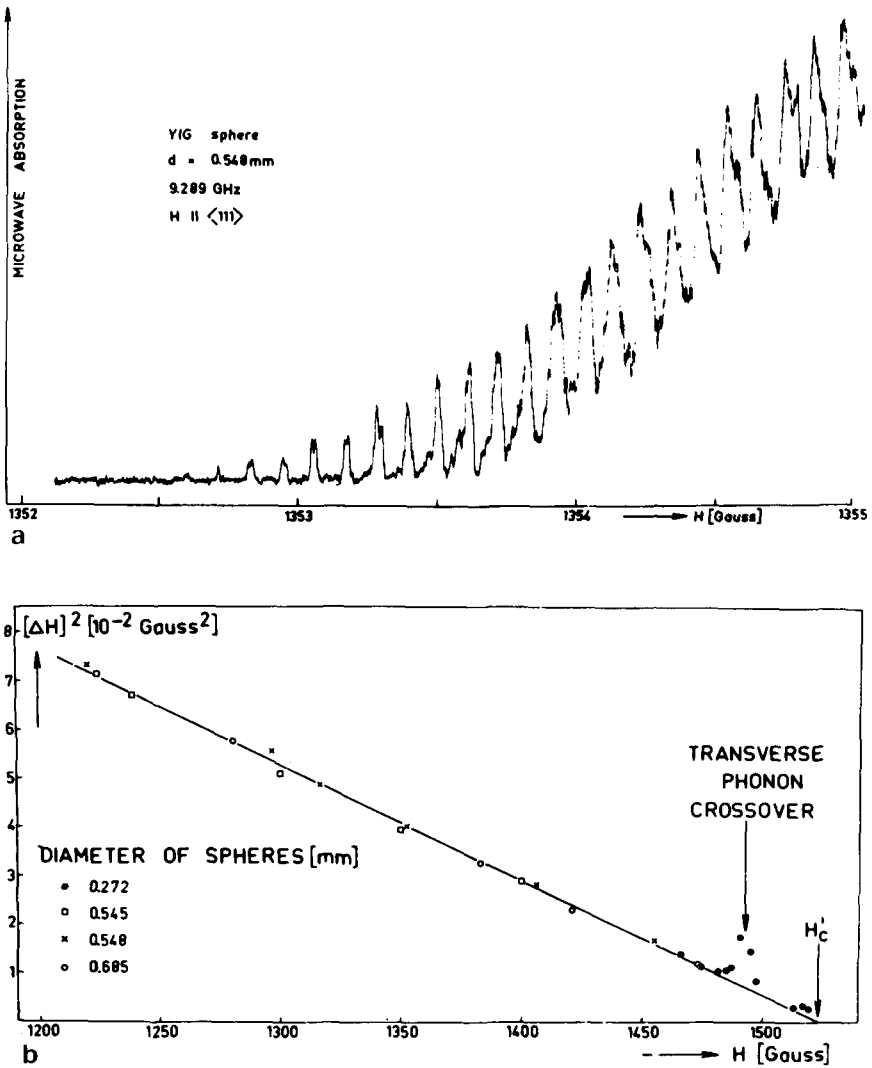

Fig. 2.(a) Absorbed microwave power versus magnetic field upon excitation of spin waves by parallel pumping in a YIG sphere (Jantz et al. 1972). (b) Intervals ΔH between absorption peaks versus magnetic field. Results obtained for four spheres of different diameters d, normalized to $d = 0.3$ mm (Jantz et al. 1972).

pumping frequencies ω_p. The relation of the wave numbers at which anomalies were observed with the SW frequencies is shown in fig. 3b. It agrees with the dispersion law of the elementary excitations with which the SW interact. The observed direct proportionality of ω to k confirms that the SW interact with

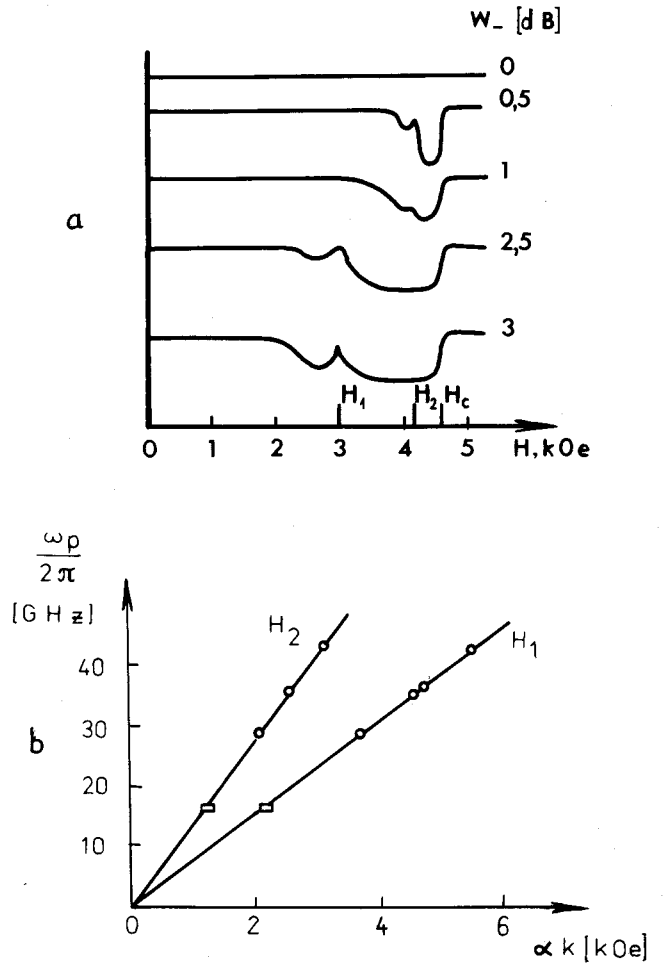

Fig. 3.(a) Absorption of microwave power in "parallel pumping" near the threshold of the parametric excitation of spin waves in $CsMnF_3$ at $T = 1.2$ K and $\omega_p/2\pi = 36$ GHz (Kotyuzhansky and Prozorova 1973). (b) Dispersion laws of the anomalies observed in fields H_1 and H_2.

sound waves. By measuring the velocity of sound, k can be determined at the point of intersection and the quantities α_i and ω_{ex} of the SW spectrum can be calculated. Table 1 lists the principal constants that characterize the properties of the objects we are interested in.

2.3.4. Spin wave damping

This quantity is an extremely important characteristic, which is, at present, of great practical significance. A detailed discussion, however, of experiments to

Table 1
Parameters of spin wave spectra for easy-plane antiferromagnets

Substance	g (GHz/kOe)	H_A (kOe)	H_E (kOe)	H_D (kOe)	H_Δ^2 (kOe^2)	$\alpha_{\parallel} \cdot 10^5$ (kOe cm)	$\alpha_{\perp} \cdot 10^5$ (kOe cm)
$CsMnF_3$	17.6	2.48	350	0	$6.4\,T$(K)	0.88	0.95
$MnCO_3$	17.6	3.04	320	4.4	$5.8/T$(K) + 0.3	0.79	0.61
$FeBO_3$	17.6	5.3	3×10^3	100	4.9	7.8	5.67

investigate the nature of the relaxation is outside the scope of our review. We shall therefore restrict ourselves to a summary of the principal relaxation processes that take place in the magnetic systems we are dealing with. At not exceedingly high $\boldsymbol{k}$, far from the Brillouin zone edge, SW damping is determined by three kinds of processes:

1. *intrinsic processes*, including three- and four-magnon relaxation, as well as relaxation of magnons due to their interaction with phonons and nuclei;

2. *two-magnon processes of elastic scattering* by inhomogeneities (pores, polycrystallinity, deviations from stoichiometry, etc.);

3. *processes proceeding with the participation of impurity ions* with strong spin–orbit coupling ("slow" and "fast" relaxation).

Quite naturally, we shall be interested chiefly in "intrinsic" relaxation, because the other contributions to damping can be substantially reduced by the selection of more perfect samples. Besides, in investigating the above-threshold state it is of great importance to know the dependence of the damping of SW on their amplitude.

The simplest and most universal method of determining $\gamma(\boldsymbol{k})$ of SW is via a calculation on the basis of the experimental values of the threshold, h_{th}, of parametric excitation of SW. The absolute accuracy of this method is not very high (the error is usually 20 to 30%). This is due to the fact that in determining the quantity γ it is necessary to employ several quantities that are usually measured with an error of several per cent. These include the power input of the resonator, the coupling coefficient with the resonator, and the quality of the resonator. Moreover, the distortion of the distribution of fields in the resonator, caused by the magnetic material, is also difficult to take into account to high accuracy. But the relative error of this method of determining damping is only 2 or 3%, making it very convenient for studies of the dependence of relaxation on various external parameters.

Calculations are carried out with eq. (12). The factor V_k in this equation depends upon the kind of magnetic system being investigated. For a cubic ferromagnet and an easy-plane AFM, these factors have been calculated by Morgenthaler (1960), Schlömann et al. (1960) and Ozhogin (1970). At present for such magnetic systems theoretical calculations are available for all relaxation processes that can occur under the conditions of actual experiments.

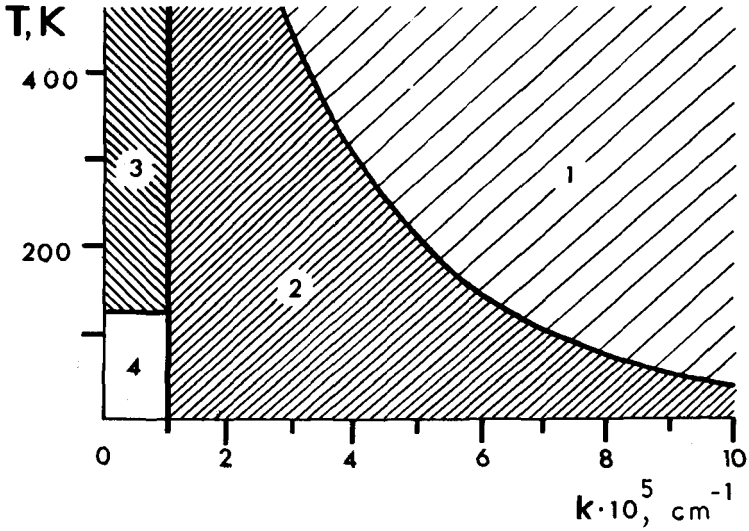

Fig. 4. Diagram of the relative contributions of various relaxation processes in YIG. Numbers indicate the regions in which the various relaxation processes predominate: 1, four-magnon; 2, three-magnon with the participation of only magnons of the quasi-ferromagnetic branch of the spectrum; 3, with the participation of optical magnons; 4, scattering by defects. Calculated for $\omega_k/2\pi = 4.7$ GHz (Kolokolov et al. 1984).

By comparing the experimentally obtained functional dependences $\gamma(\boldsymbol{k},\boldsymbol{H},T)$ with the theoretical predictions, we can separate the contributions of the various relaxation processes to the total value of γ.

It should be noted that for YIG, $MnCO_3$, $CsMnF_3$ and $FeBO_3$ there is quite satisfactory agreement between the theoretical and experimental data.

(a) *Yttrium iron garnet crystals.* The most comprehensive research of relaxation in YIG was carried out experimentally by Anisimov and Gurevich (1975, 1976) and theoretically, taking the complex magnetic structure of YIG into account, by Kolokolov et al. (1984). Figure 4 shows, in a temperature T versus wavevector k plot, the regions in which, from the theoretical viewpoint (Kolokolov et al. 1984), the contribution of one or another process predominates.

For long SW with $k < k_l$ ($ak_l \approx 2\omega_{ex}/\omega_j$), three-magnon processes in the quasi-ferromagnetic branch of the spectrum are forbidden by the conservation laws, and the amplitude of exchange four-magnon processes is very small.

The damping $\gamma(\boldsymbol{k})$ for $\boldsymbol{k} \to 0$ was first investigated experimentally by Kasuya and Le Craw (1961), who proposed that this damping is the result of a three-particle process with the participation of an optical magnon and a phonon.

The paper by Kolokolov et al. (1984) analyzed processes of this kind in detail and showed that the main contribution to the damping of SW with

$\boldsymbol{k} \to 0$ is made by a process in which a ferromagnon coalesces with optical magnons. The amplitude of this process is proportional to the uniaxial crystallographic anisotropy energy of Fe^{3+} ions at the octahedral sites a.

At low temperatures ($T < 120$ K), the damping $\gamma(0)$ decreases exponentially. In this temperature region (region 4), the main intrinsic relaxation process is four-magnon magnetic dipole scattering. But under real conditions, at $T \lesssim 120$ K and $k < k_l$, the damping of ferromagnons is, as a rule, due to defects (Grankin et al. 1975).

Magnetic dipole three-magnon relaxation predominates in region 2. It is determined by two processes, coalescence and decay,

$$\omega(\boldsymbol{k}) + \omega(\boldsymbol{k}') = \omega(\boldsymbol{k} + \boldsymbol{k}'), \tag{19}$$

$$\omega(\boldsymbol{k}) = \omega(\boldsymbol{k}') + \omega(\boldsymbol{k} - \boldsymbol{k}'). \tag{20}$$

Decay processes, eq. (20), are allowed for $k > k_m$. The quantity k_m is determined by the condition

$$\omega(k_m) = 2\omega(k_m/2). \tag{21}$$

Both in coalescence processes, eq. (19), and in decay processes, eq. (20), $\gamma(\boldsymbol{k}) \propto T$, but the dependence of γ on $\boldsymbol{k}$ differs for these processes. For $k = k_m$, a characteristic sharp turn is observed in the experimental γ versus k curve.

In region 1, the main process is four-magnon exchange scattering, and

$$\gamma(\boldsymbol{k}) = \text{const.}\ \omega(\boldsymbol{k})(ak)^2 (T/\omega_{ex})^2 \times \{\ln^2[T/\omega(\boldsymbol{k})] - 3.3 \ln[T/\omega(\boldsymbol{k})] - 0.3\} \quad \text{at } T < 200\,\text{K}, \tag{22}$$

$$\gamma(\boldsymbol{k}) = \text{const} \times \omega(\boldsymbol{k})(ak)^2 (T/\omega_{ex})^4 \quad \text{at } 200\,\text{K} < T < 350\,\text{K}.$$

In YIG at room temperature $\gamma(0) \approx 2.4 \times 10^6\,\text{s}^{-1}$, and the part of the damping depending on $\boldsymbol{k}$, for $k \approx 10^5$, is of the same order of magnitude.

(b) *Antiferromagnets with "easy-plane" anisotropy.* In the "easy-plane" (EP) antiferromagnets $MnCO_3$ and $CsMnF_3$, SW relaxation was investigated in the temperature range 1.2 to 4.2 K and in the frequency range $\omega(\boldsymbol{k})$ from 10 to 20 GHz (Kveder et al. 1972, Kotyuzhansky and Prozorova 1972, 1973). It was shown that under these conditions, $\gamma(\boldsymbol{k})$ varies between 0.1 and 10 MHz. The presence of a comparatively low-frequency $[\omega_2(0)/2\pi \approx 10^{11}\,\text{Hz}]$ quasi-antiferromagnetic (QAF) branch of the spectrum, the close magnon and phonon velocities, and the strong hyperfine interaction in AFM with Mn^{2+} ions lead to a situation in which, according to theory, SW relaxation at liquid-helium temperatures is determined by the following processes:

1. coalescence of two magnons of the QF branch into a magnon of the QAF branch, γ_{3m};
2. magnon–phonon interaction, γ_{m-ph};
3. magnon scattering by the paramagnetic subsystem of ^{55}Mn, nuclei γ_{mn}.

The relaxation parameters γ_{3m}, γ_{m-ph} and γ_{mn} have different functional dependences and, consequently, the contribution from each of these mechanisms can be separated out. The first process is the main one at relatively high temperatures and strong magnetic fields: $\gamma_{3m} \propto H^2 \exp T$. The quantity γ_{3m} coincides with the theoretical value calculated by V.L. Sobolev and given by Kotyuzhansky and Prozorova (1981). For the second process (Lutovinov 1978), $\gamma_{m-ph} \propto T\theta^2$ (where θ is the magnetoelastic interaction constant). As the temperature is lowered, SW scattering by magnetization fluctuations of the nuclear subsystem becomes predominant. As follows from theoretical considerations (Woolsey and White 1969), $\gamma_{mn} \propto AI(I+1)k/\omega_p$ (where A is the hyperfine interaction constant, I is the nuclear spin, and k is the SW wavevector). In the investigated EP antiferromagnets with Mn^{2+} ions, the value of γ_{mn} agrees with the theoretically predicted value (Andrienko and Prozorova 1985).

In this manner, the assembly of processes that were considered made it possible to describe relaxation at liquid-helium temperatures in $MnCO_3$ and $CsMnF_3$.

SW damping in $FeBO_3$ has been studied over a more extensive temperature range: from 1.2 to 150 K (Kotyuzhansky and Prozorova 1981). Measurements were made at a pumping frequency $\omega_p/2\pi = 26$ GHz, with γ varying between 1 and 50 MHz. Unfortunately, it was not possible in this case to avoid "slow relaxation", which was associated with the presence of Fe^{2+} ions, providing a maximum in γ at $T \approx 18$ K. At higher temperatures, damping is determined by three-magnon processes, at lower temperatures by magnon–phonon processes. The energy spectrum differs qualitatively from those for $MnCO_3$ and $CsMnF_3$ in that its magnon and phonon branches do not intersect, because the limiting "SW velocity" $g\alpha > v_s$ (where v_s is the velocity of sound). In this connection, in addition to coalescence processes with the participation of phonons in the range of fields in which the group velocity of magnons is less than the sound velocity, the decay process into a magnon and a phonon is allowed.

3. *S-theory: nonlinear theory of parametrically excited waves*

This and the following sections are devoted to a survey of theoretical and experimental investigations on the stationary state of a system of parametrically excited spin waves (PSW).

1962, Gottlieb and Suhl 1962), i.e., γ depends on the number of PSW,

$$\tilde{\gamma}(\boldsymbol{k}) = \gamma(\boldsymbol{k}) + \sum_{\boldsymbol{k}'} \eta(\boldsymbol{k},\boldsymbol{k}')|b_{\boldsymbol{k}'}|^2 + \cdots. \tag{23}$$

The stationary amplitudes of the waves are determined by the well-known condition of energy balance, eq. (12). For a qualitative analysis we select the simplest form of eq. (23) with $\eta(\boldsymbol{k},\boldsymbol{k}') = \eta$. Then

$$N = \sum_{\boldsymbol{k}} |b_{\boldsymbol{k}}|^2 = (hV - \gamma)/\eta = \gamma(\xi - 1)/\eta, \tag{24}$$

where supercriticality is determined by the equation

$$\xi = h/h_{\text{th}}. \tag{25}$$

As concerns the phases $\Psi(\boldsymbol{k})$, they are determined from the condition of parametric resonance, i.e., shifted by $\pi/2$ with respect to the pump phase $\Psi_{\text{p}}(\boldsymbol{k})$.

Another "phase" mechanism for amplitude limitation, proposed by Zakharov et al. (1969, 1970), plays a definite role in the parametric excitation of waves. For its discussion it is necessary to point out that the dependence of the quantity W_+ on the phase of the pair of waves [see eq. (9)] leads, even at the linear stage, to the development of parametric instability and to the establishment of a definite relationship between the phases of the waves in a pair. The phase correlation of waves with equal and oppositely directed wavevectors can be called "pairing". This term has been adopted from the BCS theory of superconductivity. In contrast to superconductivity, the physical cause leading to wave pairing is the pumping. This singles out, from the initial chaos of phases, pairs of waves for which the increment of instability is maximal. Below it will be shown that also in the nonlinear state of the instability development the phase correlation is complete. This means that even though $b_{\boldsymbol{k}}$ is a random quantity, $b_{\boldsymbol{k}}b_{-\boldsymbol{k}}$ is a dynamic quantity,

$$\sigma(\boldsymbol{k}) = \langle b_{\boldsymbol{k}}b_{-\boldsymbol{k}}\rangle = b_{\boldsymbol{k}}b_{-\boldsymbol{k}}, \qquad \langle\Psi(\boldsymbol{k})\rangle = \Psi(\boldsymbol{k}). \tag{26}$$

We shall call $\sigma(\boldsymbol{k})$ the anomalous correlation function. If $\sigma \neq 0$ energy is exchanged between pairs of waves. This exchange, depending upon the phase relations, deteriorates the coherence between the phases of the pairs and that of the external pumping, and reduces the energy flux to the PSW system. This mechanism of amplitude limitation will be discussed in detail in the following sections.

3.2. Diagonalized Hamiltonian and equations of motion in the S-theory

We simplify the interaction Hamiltonian (8) to the form

$$\tilde{\mathscr{H}}_{\text{int}} = \sum_{\boldsymbol{k},\boldsymbol{k}'} T_{\boldsymbol{k}\boldsymbol{k}'}|b_{\boldsymbol{k}}|^2|b_{\boldsymbol{k}'}|^2 + \frac{1}{2}\sum_{\boldsymbol{k}\boldsymbol{k}'} S_{\boldsymbol{k}\boldsymbol{k}'}b_{\boldsymbol{k}}^* b^*_{-\boldsymbol{k}}b_{\boldsymbol{k}'}b_{-\boldsymbol{k}'}, \tag{27}$$

where

$$T_{kk'} = T_{k'k} = T_{kk';kk'},$$

$$S_{kk'} = S^*_{k'k} = T_{k,-k;k',-k'}.$$

The only terms that have been retained in $\mathscr{H}_{\text{int}}$ are those that either do not depend upon the phases of the waves at all [first summation in eq. (27)] or depend only on the sum of the phases $\Psi(\boldsymbol{k})$ in the pairs. All other terms, depending on the phases of individual waves [more exactly on the differences $\varphi(\boldsymbol{k}) - \varphi(-\boldsymbol{k})$] have been omitted. The physical meaning of the terms retained in eq. (27) becomes clear from the equations of motion for the amplitudes b_k. After substituting the Hamiltonians (5) and (27) into eq. (3), we have

$$\{\mathrm{d}/\mathrm{d}t + \gamma(\boldsymbol{k}) + \mathrm{i}[\omega(\boldsymbol{k}) - \tfrac{1}{2}\omega_{\mathrm{p}}]\} b_k + \mathrm{i}P_k b^*_{-k} = 0. \tag{28}$$

These equations differ from linear equations, for the parametric instability only by a renormalization of the frequency $\omega(\boldsymbol{k}) \to \tilde{\omega}(\boldsymbol{k})$ and of the pumping $hV_k \to P_k$, resulting from the first and second summations in eq. (27), respectively,

$$\tilde{\omega}(\boldsymbol{k}) = \omega(\boldsymbol{k}) + 2\sum_{k'} T_{kk'} n(\boldsymbol{k}'), \qquad P_k \equiv P(\boldsymbol{k}) = hV_k + \sum_{k'} S_{kk'}\sigma(\boldsymbol{k}'), \tag{29}$$

$$n(\boldsymbol{k}) = |b_k|^2, \qquad \sigma(\boldsymbol{k}) = b_k b_{-k} = n(\boldsymbol{k}) \exp[\mathrm{i}\Psi(\boldsymbol{k})]. \tag{30}$$

Here $n(\boldsymbol{k})$ is the normal correlation function. It differs from the number of PSW by the quantum-mechanical factor $1/\hbar$. In general, in eqs. (26), it is necessary to take into account the dependence of the damping of PSW on their number, i.e. the difference between $\tilde{\gamma}$ and γ [see eq. (23)]. In the first stage of investigation we shall assume that $\tilde{\gamma} = \gamma$ and that the nonlinearity of the damping can be neglected. From eqs. (28) we obtain

$$\frac{\mathrm{d}}{\mathrm{d}t}[\varphi(\boldsymbol{k}) - \varphi(-\boldsymbol{k})] = 0. \tag{31}$$

This could be expected, because the phase difference of waves running toward one another determines the spatial position of the nodes forming a standing wave, which are not fixed in any way in a uniform pump field. This leads to a situation in which the phases φ can be brought into a chaotic state by any small interaction, for instance, by small random inhomogeneities or irregularities in the shape of the crystal. The chaotic state of the individual phases leads to a situation in which the nondiagonal terms in $\mathscr{H}_{\text{int}}$ can be neglected in the first-order approximation of the theory. A more detailed and rigorous justification of the approximation of the diagonal Hamiltonian (27) is given by L'vov (1975) and will be discussed in section 3.6.2. Here we only point out that this approximation is valid right up to the amplitude of the pump field, i.e. $h < h_*$, where

$$h_* = h_{\text{th}}(kv/\gamma)^{1/2} \gg h_{\text{th}}, \quad \boldsymbol{v}(\boldsymbol{k}) = \partial\omega(\boldsymbol{k})/\partial\boldsymbol{k}. \tag{32}$$

3.3. Ground state in the S-theory. Condition of external stability

We begin by considering the stationary states of a system of pairs of waves, in which the quantities $n(\boldsymbol{k})$ and $\Psi(\boldsymbol{k})$ are time independent. Setting $\dot{b}_k = 0$ in eq. (28), we immediately obtain the condition

$$\{|P(\boldsymbol{k})|^2 - \gamma(\boldsymbol{k})^2 + [\tilde{\omega}(\boldsymbol{k}) - \tfrac{1}{2}\omega_p]^2\}\, n(\boldsymbol{k}) = 0.$$

For $|P(\boldsymbol{k})| > \gamma(\boldsymbol{k})$ this equation has two solutions, determining two surfaces in $\boldsymbol{k}$-space on which $n(\boldsymbol{k})$ may be nonzero,

$$\tilde{\omega}(\boldsymbol{k}) = \tfrac{1}{2}\omega_p \pm [|P(\boldsymbol{\Omega})|^2 - \gamma(\boldsymbol{\Omega})^2]^{1/2}. \tag{33}$$

Here we neglected the unimportant dependence of P and γ on $|\boldsymbol{k}|$, leaving only their dependence on the direction of the vector $\boldsymbol{\Omega} = \boldsymbol{k}/k$. We point out that there is an uncountable set of stationary states, differing both in the function $P(\boldsymbol{\Omega})$ specifying the surfaces of eq. (33), and in the distribution of $n(\boldsymbol{k})$ on them. As a matter of fact, the direction of $\boldsymbol{\Omega}$, at which $n(\boldsymbol{k})$ vanishes, can be specified arbitrarily.

Of all the stationary states only those can actually be realized that are stable with respect to small perturbations. The requirement of stability drastically reduces the class of possible stationary states. Let us investigate the stability with respect to the creation of a pair of waves outside the surfaces of eq. (33); this is the so-called "external stability". For this purpose we write, with the aid of eq. (28), an equation for a pair of perturbing waves $b(\boldsymbol{q},t) \propto \exp \nu(\boldsymbol{q})t$ and $b^*(\boldsymbol{q},t) \propto \exp \nu(\boldsymbol{q})t$ and obtain the expression for $\nu(\boldsymbol{q})$ in the usual way,

$$\nu(\boldsymbol{q}) = -\gamma(\boldsymbol{\Omega}) + \{|P(\boldsymbol{\Omega})|^2 - [\tilde{\omega}(\boldsymbol{q}) - \tfrac{1}{2}\omega_p]^2\}^{1/2}. \tag{34}$$

The condition of external stability, $\nu < 0$, can, in this way, be written in the form

$$|P(\boldsymbol{\Omega})| \leqslant \gamma(\boldsymbol{\Omega}). \tag{35}$$

On the other hand, it follows from eq. (33) that $|P(\boldsymbol{\Omega})| > \gamma(\boldsymbol{\Omega})$ for the directions of $\boldsymbol{k}$ in which $n(\boldsymbol{k}) \neq 0$. Consequently, for these directions the two inequalities are compatible only for $|P(\boldsymbol{\Omega})| = \gamma(\boldsymbol{\Omega})$, when the two surfaces of eq. (33) coalesce into one,

$$2\tilde{\omega}(\boldsymbol{k}) = \omega_p. \tag{36}$$

Hence, the condition of external stability for a given distribution of wave amplitudes with respect to angles completely eliminates the arbitrariness in selecting the surface on which $n(\boldsymbol{k}) \neq 0$. We shall call this surface, eq. (36), the "resonance surface", and the stationary state, that has external stability, the "ground state".

The result here obtained has a simple physical meaning. As is evident from eq. (28), in the linear state, the waves with a frequency detuning equal to zero are most strongly coupled to the pump field. The quantity $\tilde{\omega}(\boldsymbol{k}) - \omega_p/2$

represents the frequency detuning with nonlinear terms taken into account. If the two surfaces of eq. (33) on which $n(\boldsymbol{k}) \neq 0$ do not coalesce into one, then the SW pairs that get into the spherical layer between them are more strongly coupled to the pump field than the ones we already have, and they will be excited; this is what instability means.

3.4. The simplest stationary solutions in the S-theory

We introduce the distribution function $N(\boldsymbol{\Omega})$ of the "number" of pairs per unit solid angle. Defining $N(\boldsymbol{\Omega})$ by the equation

$$N = \sum_{k} n(\boldsymbol{k}) = \int N(\boldsymbol{\Omega})\, \mathrm{d}\boldsymbol{\Omega}, \quad \mathrm{d}\boldsymbol{\Omega} = \sin\vartheta\, \mathrm{d}\vartheta\, \mathrm{d}\varphi, \tag{37}$$

we rewrite the stationary equation for $N(\boldsymbol{\Omega})$ and $\Psi(\boldsymbol{\Omega})$, following from eqs. (28), (29) and (36), in the form

$$\{P(\boldsymbol{\Omega}) \exp[-\mathrm{i}\Psi(\boldsymbol{\Omega})] - \mathrm{i}\gamma(\boldsymbol{\Omega})\} N(\boldsymbol{\Omega}) = 0,$$

$$P(\boldsymbol{\Omega}) = hV(\boldsymbol{\Omega}) + \int S(\boldsymbol{\Omega},\boldsymbol{\Omega}') N(\boldsymbol{\Omega}') \exp[\mathrm{i}\Psi(\boldsymbol{\Omega}')]\, \mathrm{d}\boldsymbol{\Omega}'. \tag{38}$$

These equations do not yet define the distribution of PSW uniquely, because regions in which $N(\boldsymbol{\Omega}) = 0$ can be arbitrarily specified on the surface. The requirement of external stability, as shall be shown in the following, substantially reduces the class of possible solutions, and in many cases only stable distributions remain.

We shall begin our investigation of these equations with the simplest spherically symmetric case, which is realized, for example, in AFM (neglecting exceptionally small magnetic dipole interaction). For $V(\boldsymbol{\Omega}) = V$, $\gamma(\boldsymbol{\Omega}) = \gamma$ and $S(\boldsymbol{\Omega},\boldsymbol{\Omega}') = S$, eqs. (38) have the isotropic solution $N(\boldsymbol{\Omega}) = N/4\pi$, for which

$$|S|N = [(hV)^2 - \gamma^2]^{1/2}, \qquad hV \sin\Psi = \gamma. \tag{39}$$

These equations have the same kind of solution if $S_{kk'}$ depends only on the angle between $\boldsymbol{k}$ and $\boldsymbol{k}'$. Then in eq. (39)

$$4\pi S = \int S(\boldsymbol{\Omega},\boldsymbol{\Omega}')\, \mathrm{d}\boldsymbol{\Omega}'. \tag{40}$$

Also of great interest is the axially symmetric case, which is realized in an isotropic and cubic ferromagnet, magnetized along the (111) or (100) axis, for instance, in YIG. Here the coefficient of the coupling with the pump field and the coefficients describing the interaction are of the form

$$V(\boldsymbol{\Omega}) = V(\vartheta) \exp(2\mathrm{i}\varphi), \quad V(\vartheta) = V \sin^2\vartheta,$$

$$S(\boldsymbol{\Omega},\boldsymbol{\Omega}') = S(\vartheta,\vartheta',\varphi - \varphi'), \qquad T(\boldsymbol{\Omega},\boldsymbol{\Omega}') = T(\vartheta,\vartheta',\varphi - \varphi'). \tag{41}$$

It is clear from the axial symmetry that in the stationary state $N(\Psi)$ is independent of the azimuthal angle φ. We determine the amplitude $N(\vartheta)$ and the "invariant" phase $\Psi(\vartheta)$ of the pair by the equations

$$2\pi N(\vartheta) = N(\Omega), \qquad \Psi(\Omega) = \Psi(\vartheta) + 2\varphi. \tag{42}$$

Then eq. (38) is simplified to the form

$$\{P(x)\exp[-i\Psi(x)] - i\gamma(x)\}N(x) = 0, \qquad x = \cos\vartheta,$$

$$P(x) = P(\Omega)\exp 2i\varphi = hV(x) + \int S(x,x')N(x')\exp[i\Psi(x')]\,dx', \tag{43}$$

$$2\pi S(x,x') = \int S(\Omega,\Omega')\exp[2i(\varphi - \varphi')]\,d\varphi'. \tag{44}$$

It is readily evident that slightly above the threshold, the function $N(x)$ is nonzero at $x = 0$, i.e. only at the "equator" of the resonance surface:

$$N(x) = N_1\delta(x) \propto \delta(\vartheta - \pi/2). \tag{45}$$

For N_1 and phase $\Psi_1 = \Psi(0)$ we readily obtain from eq. (43)

$$(S_{11}N_1)^2 = (hV_1)^2 - \gamma_1^2, \qquad hV_1\sin\Psi_1 = \gamma_1, \tag{46}$$

where $V_1 = V(x)$, $S_{11} = S(x,x)$, and $\gamma_1 = \gamma(x)$ at $x = 0$. An essential property of the solutions obtained is that the phase of the pairs, $\Psi = \varphi(\boldsymbol{k}) + \varphi(-\boldsymbol{k}) + \Psi_p$ (Ψ_p is the pump phase, which is usually taken to be equal to zero), differs from the value $\pi/2$ at which the flux of energy W_+ from the external pump field [see eq. (9)] is maximal. Condition (46) describes the energy balance typical for the phase mechanism of limitation of the amplitude of SW.

3.5. *Stage-by-stage excitation of waves*

We shall now investigate the distribution $N(\Omega)$ of PSW over the resonance surface when the amplitude of the external field h is increased. A general theorem can be proved (Zakharov et al. 1970) showing that for sufficiently low supercriticality, $N(\Omega)$ is nonzero only in the directions in which $|V(\Omega)|/\gamma(\Omega)$ is maximal. For spherical symmetry, these points lie all over the surface; for axial symmetry, they lie on one ($\vartheta = \pi/2$) or two lines. In cases of lower symmetry, there are one or several equivalent pairs of points. It is of interest that the integral amplitude is only slightly sensitive to the type of symmetry of the problem. It is determined by eq. (46), in which $V_1 = \max|V(\Omega)|$, and S_{11} is the average value of $S(\Omega,\Omega')$ over a set of points with $N(\Omega) \neq 0$.

It can be shown that the pair distribution function (45), concentrated on the equator, retains its stability with respect to pair creation at other latitudes right up to sufficiently strong fields $h < h_2$. For $h = h_2$ a second group of pairs is created with $\vartheta = \vartheta_2$. Estimates by Zakharov et al. (1974) yield $h_2/h_{th} \gtrsim 3$ and $\vartheta_2 \approx 50°$. Of much more importance, however, than the numerical values

of h_2 and ϑ_2 is the fact itself of the consecutive, stage-by-stage excitation of wave packets singular in $\boldsymbol{k}$-space. This qualitative conclusion of the S-theory was confirmed by a direct experiment by Zautkin et al. (1970), in which the second threshold was observed in YIG (see section 4).

We conclude this subsection with a description of the quantitative behavior of PSW for $h > h_2$. It can be shown that a state with two groups of pairs at the latitudes ϑ_1 and ϑ_2 becomes unstable at a certain field h_3, and a third group is created at latitude ϑ_3. At h_4 the next group at latitude ϑ_4 is created, etc. The question of what happens upon a further increase of h was discussed by Zakharov et al. (1970). For high values of h, the distribution $N(\vartheta)$ is very sensitive to the fine structure of the quantities $V(\boldsymbol{\Omega})$ and $S(\boldsymbol{\Omega},\boldsymbol{\Omega}')$; in some cases a continuous distribution of pairs is established, whereas in others an essentially nonstationary pattern appears.

3.6. S, T^2-theory and fine structure of the distribution function for parametric waves with respect to $\boldsymbol{k}$ and ω

3.6.1. Basic equations

Recall that the S-theory only takes coordinated interaction of pairs in first order of perturbation theory with respect to $\mathscr{H}_{\text{int}}$ into account. The next effect that must be included in a more detailed theory is the scattering of PSW by one another, which is proportional to the second power of the matrix element $T_{12,34}$ in $\mathscr{H}_{\text{int}}$. In the S, T^2-theory, which takes both effects into account, a finite width of the PSW packet appears, both with respect to the magnitude of $\boldsymbol{k}$ [and, correspondingly, with respect to the inherent wave frequencies $\omega(\boldsymbol{k})$] and with respect to the actual wave frequencies ω. To describe the distribution of PSW packets with respect to $\boldsymbol{k}$ and ω, it is necessary to make use of the correlation functions $n(q)$ and $\sigma(q)$:

$$\langle a(q)a^*(q')\rangle = n(q)\delta^4(q - q'), \quad q = (\boldsymbol{k},\omega),$$
$$\langle a(q)a(q')\rangle = \sigma(q)\delta^4(q - \bar{q}'), \quad \bar{q} = (-\boldsymbol{k},\omega_{\text{p}} - \omega), \tag{47}$$

where $a(q) = a(\boldsymbol{k},\omega)$ is the Fourier transform of $a(\boldsymbol{r},t)$. Unfortunately, it is impossible to formulate closed equations of motion for the quantities in eq. (47). Also inevitably included in the S, T^2-theory are two Green's functions: the normal Green's function $G(q)$ and the anomalous Green's function $L(q)$, describing the reaction of the PSW system to an external force $f(q)$,

$$\langle \delta a(q)/\delta f(q')\rangle = G(q)\delta^4(q - q'),$$
$$\langle \delta a(q)/\delta f^*(q')\rangle = L(q)\delta^4(q - \bar{q}'). \tag{48}$$

A systematic derivation of the equations of the S, T^2-theory, making use of the diagram technique for nonequilibrium processes, was carried out by L'vov (1975). In this paper a system of Dyson–Wyld equations is obtained, as a

result of the summation of weakly bound diagrams,

$$G(q) = -[\omega + \tilde{\omega}(\boldsymbol{k}) - \omega_p + i\gamma(\boldsymbol{k})]\Delta^{-1}(q),$$

$$L(q) = P(q)\Delta^{-1}(q), \quad P(q) = P(\boldsymbol{k}) + \text{terms} \propto T^2, T^3, \text{etc.}$$

$$\Delta(q) = [\omega + \tilde{\omega}(\boldsymbol{k}) - \omega_p + i\gamma(\boldsymbol{k})][\tilde{\omega}(\boldsymbol{k}) - \omega - i\gamma(\boldsymbol{k})] - |P(q)|^2, \tag{49}$$

$$n(q) = [|G(q)|^2 + |L(q)|^2]\Phi(q) + G(q)\tilde{\Psi}(q)L^*(\bar{q}) + L(q)\tilde{\Psi}^*(q)G^*(q),$$

$$\sigma(q) = G(q)L(q)\Phi(q) + L(\bar{q})G(\bar{q})\Phi(\bar{q}) + G^2(q)\tilde{\Psi}(\bar{q}) + L^2(q)\tilde{\Psi}^*(q), \tag{50}$$

$$\Phi(q) = 2\int \{|T_{k1,23}|^2 n_1 n_2 n_3 + 2T_{k1,23}T_{k2,13}\sigma_1^\dagger \sigma_2 n_3\}$$
$$\times \delta^4(q + q_1 - q_2 - q_3)\,d^4q_1\,d^4q_2\,d^4q_3 + \cdots, \tag{51}$$

where $\cdots$ stands for terms $\propto T^3$, $\propto T^4$, etc. The expressions for P, Φ and $\tilde{\Psi}$ are partially summed but, nevertheless, are infinite series of perturbation theory. If, however, the wave amplitudes are not too large, it proves sufficient to restrict oneself to the first few diagrams. In S,T^2-theory we restrict ourselves to diagrams of second order in the wave interaction in the expressions for Φ and $\tilde{\Psi}$, and of first order in the expression for P and $\tilde{\omega}(\boldsymbol{k})$. A general quantative analysis of the system of integral equations (49), (50) and (51) is an extremely complex and cumbersome problem. We shall therefore describe its results only for certain limiting cases, enabling us to obtain a qualitative idea of the situation.

3.6.2. Role of thermal noise in the S-theory

With relatively small numbers N of PSW, the main contribution to Φ is made by "thermal" spin waves (TSW), i.e. SW that do not interact with the pump field. To first order it can be assumed that they are in thermodynamic equilibrium. Then

$$\Phi(q) = \Phi_0(\boldsymbol{k}) = \gamma(\boldsymbol{k})n_0(\boldsymbol{k})/\pi, \tag{52}$$

where $n_0(\boldsymbol{k})$ is an equilibrium function of the TSW distribution,

$$n_0(\boldsymbol{k}) = \hbar\{\exp[\hbar\omega(\boldsymbol{k})/T] - 1\}^{-1}. \tag{53}$$

With equations (49), (50) and (52) the effect of all equilibrium TSW on the system of PSW can be analyzed within the framework of the S-theory. It is first of all necessary to note the finiteness of the width of the PSW packet with respect to ω near $\omega_p/2$,

$$\Delta\omega = v^2(\boldsymbol{k})/2\gamma(\boldsymbol{k}), \quad v^2(\boldsymbol{k}) = \gamma^2(\boldsymbol{k}) - |P(\boldsymbol{k})|^2. \tag{54}$$

Integrating eq. (50) over ω, we readily obtain

$$n(\boldsymbol{k}) = n_0(\boldsymbol{k})|P(\boldsymbol{k})|^2\Delta(\boldsymbol{k})^{-1},$$

$$\Delta(\boldsymbol{k}) = [\tilde{\omega}(\boldsymbol{k}) - \omega_p/2]^2 + \nu(\boldsymbol{k})^2, \tag{55}$$
$$\sigma(\boldsymbol{k}) = n_0(\boldsymbol{k})[\tilde{\omega}(\boldsymbol{k}) - \omega_p/2 + i\gamma(\boldsymbol{k})]\Delta(\boldsymbol{k})^{-1}.$$

It is evident that the distribution of $n(\boldsymbol{k})$ and $\sigma(\boldsymbol{k})$ with respect to the magnitude of $\boldsymbol{k}$ is of the form of a Lorentz function with a maximum on the resonance surface of eq. (36) and half-width $\nu(\boldsymbol{k})$. This quantity is readily estimated by integrating eq. (55) over the magnitude of $\boldsymbol{k}$,

$$\Delta\omega(\boldsymbol{k}) = \nu(\boldsymbol{k}), \quad \nu(\boldsymbol{k}) = N_T|P|^2/Nkv, \quad N_T = n_0 k^3/(2\pi)^2. \tag{56}$$

Here N_T is, in order of magnitude, the number of thermal SW in a sphere of radius k, and $v(k)$ is the group velocity of SW. Equation (55) can similarly be transformed into the form

$$\gamma(\boldsymbol{k})[n(\boldsymbol{k}) - n_0(\boldsymbol{k})] + \mathrm{Im}\{P^*(\boldsymbol{k})\sigma(\boldsymbol{k})\} = 0,$$
$$\{\gamma(\boldsymbol{k}) + i[\tilde{\omega}(\boldsymbol{k}) - \omega_p/2]\}\sigma(\boldsymbol{k}) + iP(\boldsymbol{k})n(\boldsymbol{k}) = 0. \tag{57}$$

These equations differ from the equations of the *S*-theory only by the nonuniform term γn_0, which describes the effect of thermal fluctuations on the PSW system. It follows, in particular, from these equations that for spherical symmetry of the problem and above the threshold, i.e. for $h/h_{th} - 1 > \varepsilon$ (Zakharov and L'vov 1971),

$$SN = \gamma(\xi^2 - 1)^{1/2}[1 + \varepsilon^2/2(\xi^2 - 1)^2],$$
$$\nu^2 = \varepsilon^2\gamma^2/(\xi^2 - 1), \quad \xi = h/h_{th}. \tag{58}$$

Here $\varepsilon = SN_T/kv \ll 1$ is the small parameter of the problem and characterizes the effect of thermal fluctuations. Thus, the quantity N differs little from that predicted by the *S*-theory [see eq. (46)]. The basic difference from the *S*-theory lies in the finite width $n(\boldsymbol{k})$ of the packet of waves with respect to the magnitude of $\boldsymbol{k}$, resulting from the action of the thermal fluctuations of the medium. For $\xi - 1 > \varepsilon$, this width, however, as follows from eq. (56), is small: $\nu < \gamma$. Expression (58) was also obtained by Mikhailov (1975) by means of the random forces method.

3.6.3. Role of scattering of parametrically excited spin waves by one another

The nondiagonal terms in $\mathscr{H}_{int}$, omitted in the *S*-theory, describe PSW scattering on one another. It can be shown that with not excessively high pump fields $h < h_*$ [see eq. (32)] the role of these processes is analogous to that of thermal noise; they practically have no effect on the integral characteristics of PSW, which are correctly described by the *S*-theory, and lead only to a broadening of the PSW packet with respect to ω and $\boldsymbol{k}$.

(a) *Broadening of a parametrically excited spin wave packet with respect to frequencies.* We shall describe here the case that is simplest to investigate, with

strong two-magnon scattering in the magnetic system, which is due to random inhomogeneities, defects, etc. If the damping γ_{el} of two-magnon scattering substantially exceeds the damping γ resulting from inherent processes of magnon relaxation, the distribution function $n(\boldsymbol{k})$ is isotropic, i.e. independent of the direction of $\boldsymbol{k}$ (Zakharov and L'vov 1971). The distribution with respect to the magnitude of $\boldsymbol{k}$ is the square of the Lorentz function with width $\Delta\omega_k = \gamma_{el}$; the distribution with respect to ω is described by the following equation (Krutsenko et al. 1978):

$$N(\omega) \propto \cosh^{-1}[(2\omega - \omega_p)/\eta], \quad N(\omega) = \int n(\boldsymbol{k}, \omega)\, d^3\boldsymbol{k}. \tag{59}$$

An estimate of the width of the packet, η, is given by the equation

$$\eta \approx \gamma(\gamma_{el}/\gamma)^2[(kv/\gamma)(\xi^2 - 1)]^{1/2}.$$

(b) *Broadening of a parametrically excited spin wave packet with respect to the magnitude of* $\boldsymbol{k}$. In contrast to thermal noise, when the shape of the PSW packet with respect to the magnitude of $\boldsymbol{k}$ is Lorentzian, the scattering of PSW by one another leads to different dependence of $n(\boldsymbol{k})$ on $|\boldsymbol{k}|$: the square of the Lorentz function (L'vov 1975). This is especially evident if we substitute $\omega = \omega_p/2$ into eqs. (49) and (50).

To estimate the width of the packet it is sufficient to integrate these equations over the magnitude of $\boldsymbol{k}$. As a result we obtain (L'vov 1975) $\Delta\omega_k = \nu$, where

$$(\nu/\gamma)^3 \approx (TN)^2/\gamma kv \approx (\gamma/kv)(\xi^2 - 1). \tag{60}$$

It is evident from eqs. (48) and (49) that the relative difference between their coefficients and those of the equations of the S-theory are small with respect to the parameter $(\nu/\gamma)^2$ and, consequently, with respect to this same parameter there is little difference between the results of the S-theory for the integral value of N and the exact results of the S, T^2-theory. It follows from eq. (48), in particular, that $1 - |\sigma|/n \approx \nu^2/2\gamma$, i.e., for $\nu \ll \gamma$ the phase correlations in pairs of waves are almost completely conserved. An estimate of the expressions omitted in the S, T^2-theory [see eq. (51)], which are proportional to T^3, T^4, etc., indicates that they are small with respect to powers of the parameter λ, where

$$\lambda \approx \gamma TN/vkv \approx (\gamma TN)^{1/3}/(kv)^{2/3} \ll 1 \quad \text{for } h \leqslant h_*.$$

This means that right up to a field $h \approx h_*$, determined from the condition $\nu \approx \gamma$ [see eq. (32)], the equations of the S, T^2-theory are valid, and the integral quantities N, χ' and χ'' are well described by the corresponding equations of the S-theory. It is necessary, however, to point out that, due to unexpected cancellations, the estimates obtained for ν, $\Delta\omega$ and $\Delta\omega_k$ may not turn out to be valid in certain specific situations. Therefore, notwithstanding the clarity in principle of the basic propositions of the S, T^2-theory, the investigation of the

parametric excitation of waves in other media can still lead to the discovery of new effects.

3.7. Nonlinear damping mechanisms

In SW damping calculations it is assumed that the SW distribution $n(\boldsymbol{k})$ is a thermodynamical equilibrium distribution, i.e. $n(\boldsymbol{k}) = n_0(\boldsymbol{k})$. For PSW this is only true when their number N is substantially less than the total number N_T of thermal SW (TSW), with which they interact. If, however, N becomes equal to N_T, then $n(\boldsymbol{k})$ differs essentially from $n_0(\boldsymbol{k})$, and the PSW damping $\tilde{\gamma}(\boldsymbol{k})$ begins to depend substantially on their number, i.e. nonlinear damping (ND) results. Similar ideas on the mechanisms of ND had been advanced long ago by Gottlieb and Suhl (1962), Le Gall et al. (1967), and Melkov (1971), but an accurate calculation of ND was carried out only relatively recently: for the FM YIG by L'vov and Fal'kovich (1982) and for AFM by Lutovinov and Savchenko (1977), Mikhailov and Farzetdinova (1981), and Mikhailov and Chubukov (1984).

(a) *YIG*. Of importance in this FM for various k values is one of three nonlinear damping (ND) mechanisms. For low k values (large H) the main mechanism is a negative ND, due to the coalescence of PSW with TSW. This contribution of ND (curve 1 in fig. 5) depends only comparatively weakly on the magnetic field for $H < H_1$, where $gH_1 \approx 4\omega_p/9 - \omega_m/6$. Positive ND, due to PSW decay into two TSW (curve 3), is considerable for $H \leqslant H_3$, when $k \geqslant k_m$ and these processes are allowed by the conservation laws [see eq. (21)]. The third ND mechanism, associated with the coalescence of two PSW into one TSW, plays a relatively small role. It is observable only in a narrow range of fields near H_{3m} (where H_{3m} is the upper boundary of the range of fields in which this process is allowed). The resulting dependence of the coefficient η of ND on the field in YIG [at $T = 300$ K and $\omega(k) = 5$ GHz] is given in fig. 5.

(b) *$FeBO_3$*. As has already been noted, the main contribution to PSW damping in this easy-plane AFM is made by the decay of PSW into a phonon and TSW. This process leads also to positive ND, which was calculated by Mikhailov and Chubukov (1984). The obtained dependence of the quantity η for low values of H is proportional to $1/T$ and in order of magnitude coincides with that experimentally measured at liquid-helium temperatures by Kotyuzhansky and Prozorova (1984). Other ND mechanisms, discussed by Lutovinov and Savchenko (1977) and Mikhailov and Farzetdinova (1983), make a substantially smaller contribution at low temperatures.

(c) *$MnCO_3$ and $CsMnF_3$*. Decay processes are forbidden in these easy-plane AFM, and there is no positive ND. As to the negative ND observed in

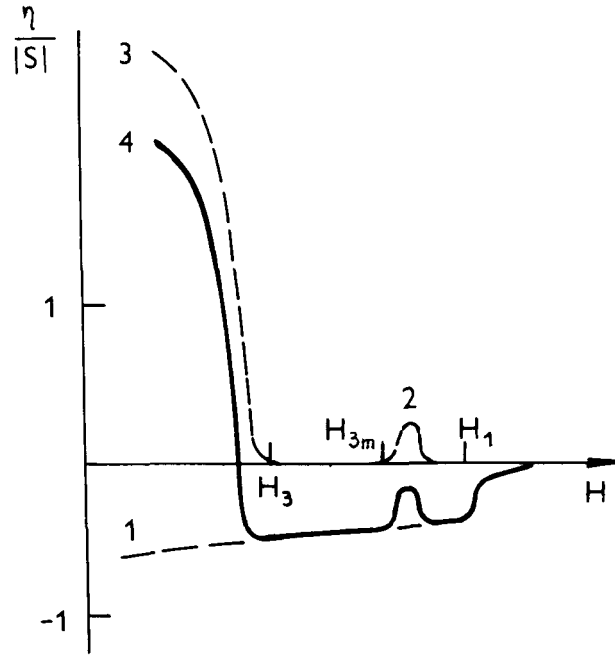

Fig. 5. Coefficient of SW nonlinear damping in YIG versus magnetic field: 1, coalescence of PSW and TSW; 2, coalescence of two PSW; 3, decay; 4, total dependence (L'vov and Fal'kovich 1982).

experiments conducted by Kveder et al. (1972), Kotyuzhansky and Prozorova (1971), and Ozhogin and Yakubovsky (1974), its physical nature is not yet clear.

3.8. Effect of nonlinear damping on the behavior of parametrically excited spin waves

3.8.1. Number of parametrically excited spin waves and phase of pairs of waves

Assume for simplicity that $\eta(\boldsymbol{k}, \boldsymbol{k}')$ depends only weakly on $\boldsymbol{k}$ and $\boldsymbol{k}'$, and that for narrow PSW packets it can be assumed that $\eta(\boldsymbol{k}, \boldsymbol{k}') = \eta$. Then, in accordance with eqs. (24) and (9), we can obtain, instead of eq. (39), for one group of pairs

$$N = \gamma \frac{-\eta \pm [S^2(\xi^2 - 1) + \eta^2 \xi^2]^{1/2}}{\eta^2 + S^2},$$

$$\cos \Psi = -SN/hV. \tag{61}$$

For $\eta \ll S$, eq. (61) transforms into eq. (39), and for $S \ll \eta$ into eq. (25).

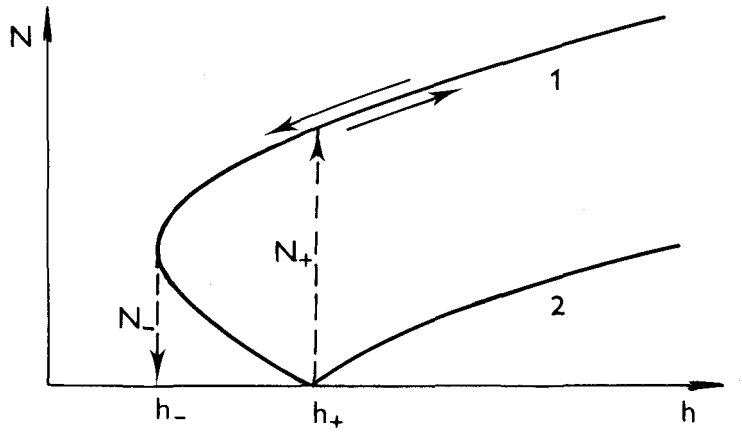

Fig. 6. Theoretical dependence of the number N of PSW on the amplitude of the microwave field in the case when there is negative nonlinear damping in the system.

If ND is negative, then parametric excitation of SW is hard and is accompanied by hysteresis (see curve 1 in fig. 6). The magnitudes of the foreward, N_+, and backward, N_-, jumps are determined by the equations

$$2N_- = N_+ = 2\gamma|\eta|/(\eta^2 + S^2),$$
$$h_+V = \gamma, \qquad h_-V = \gamma|\eta|/\sqrt{\eta^2 + S^2}. \tag{62}$$

With a positive ND, SW excitation is soft (curve 2). For small supercriticality

$$N = \frac{\gamma}{\eta}(\xi - 1), \qquad \cos\Psi = -\frac{S}{\eta}\left(\frac{\xi - 1}{\xi}\right). \tag{63}$$

It can be seen that for $\eta > S$ the phase Ψ of the pairs of waves deviate little from $\pi/2$.

3.8.2. Width of a parametrically excited spin wave packet with respect to wavevector and frequency

In accordance with eqs. (54) and (56), the width of a PSW packet with respect to $\boldsymbol{k}$, $\Delta\omega_k$, and ω, $\Delta\omega$, is determined by the quantity ν, whose dependence on the supercriticality (in limiting the number of PSW ND mechanisms) is readily determined by substituting $P = hV = \tilde{\gamma} = \gamma + \eta N$ into eq. (56). As a result of this substitution we obtain (Mikhailov and Chubukov 1984)

$$\Delta\omega_k = \beta\gamma\xi^2(\xi - 1)^{-1}, \qquad \Delta\omega = \beta^2\gamma\xi^3(\xi - \phi)^{-2}, \tag{64}$$

where $\beta = \eta N_T/kv \ll 1$. It should be understood, however, that these expressions have a limited validity because in their derivation the interaction of

secondary SW with one another and their nonlinear damping were not taken into account.

4. Experimental investigations of the stationary above-threshold state

4.1. Stage-by-stage excitation

As has been shown in section 3.5, one of the main conclusions of the *S*-theory is the stage-by-stage excitation of wave packets that are singular in $\boldsymbol{k}$-space. This means that when the microwave power is smoothly increased, first a narrow wave packet is excited, for which h_{th} is minimal. When the power is further increased, this packet is not broadened. Only when the microwave field reaches a strength h_2 exceeding h_{th} by 8 to 10 dB, another group of waves is created discontinuously. The observation of the influence of the size effect and of magnon–phonon peaks on the relation $h_{\text{th}}(\boldsymbol{H})$ is an indication that this conclusion is correct.

Zautkin et al. (1970) found direct experimental proof of this proposition. A YIG sample was put into a cylindrical resonator with two degenerate orthogonal modes (TE_{112}). magnetic fields of which, $h_{\parallel}$ and $h_{\perp}$, were parallel and perpendicular to the static field $\boldsymbol{H}$, respectively. The required polarization of the modes and their decoupling was achieved by a definite orientation of the waveguides that connect the resonator with the generator and input device.

The parallel channel ($h_{\parallel}$) was used for the parametric excitation of SW pairs with frequency $\omega(\boldsymbol{k})/2\pi = 4.7$ GHz; the perpendicular channel ($h_{\perp}$) served to register the radiation of the sample at the pump frequency $\omega_{\text{p}} = 2\omega(\boldsymbol{k})$. Up to the SW excitation threshold, the decoupling between the channels was 55 dB. A drastic increase in radiation power was observed (fig. 7) in the perpendicular channel at a supercriticality $\xi \approx 8$–12 dB. (Different values of ξ are due to variations in the constant field, and the orientation and shape of the samples.) The radiation in the perpendicular channel is the result of the interaction of SW pairs $a_{\pm k}$ with the uniform precession a_0 of the magnetization, which is described by the Hamiltonian

$$\mathscr{H}_{\perp} = \frac{1}{2}\sum_{k} (u_k^* a_0^* a_k a_{-k} + \text{c.c.}), \tag{65}$$

where $u_k = u \sin(2\vartheta)\ \exp(i\varphi)$. The radiation power is determined by the expression

$$P_{\perp}^2 = h_{\perp}^2 \propto \left| \sum_{k} u_k^* a_k a_{-k} \right|^2, \tag{66}$$

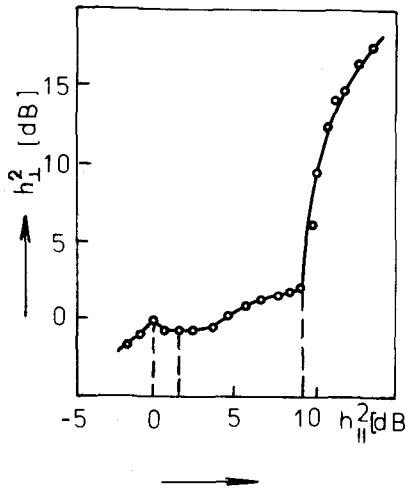

Fig. 7. Radiation power in a transverse channel versus pump power for a YIG sphere: $\omega_p/2\pi = 9.4\,\text{GHz}$, $H = 1600\,\text{Oe}$, $\boldsymbol{H}\|[100]$ (Zautkin et al. 1970).

which vanishes for $\vartheta = 0$ and $\vartheta = \pi/2$. The dependence $P_\perp(h_\parallel)$, plotted in fig. 7, is conclusive evidence that in the ξ range from 0 to 8 dB, only SW pairs propagating at an angle $\vartheta = \pi/2$ are excited. The radiation appearing at higher supercriticalities is naturally associated with the excitation of a second group of pairs with $\vartheta \neq \pi/2$. The presence of a second threshold can also be observed by the characteristic distortion of the pump pulse. A series of consecutive thresholds, first observed in this manner by Petrakovsky and Berzhansky (1970) in YIG, is evidently associated with the stage-by-stage excitation of parametric SW.

4.2. Investigation of the phase detuning of parametrically excited spin waves

For the investigation of the stationary state, Prozorova and Smirnov (1974, 1975) developed the "method of transient processes". The essence of this method is as follows. In the stationary state, the PSW system is in equilibrium with the pump field incident on the sample. A rapid variation of the pump parameters (phases, frequencies and amplitudes) compared with the SW lifetime leads to a violation of equilibrium and to a change in the absorbed power. Then a certain transient process is observed and during the time $\tau = 1/2\gamma$ the system again reaches a stationary state. The properties of the stationary state can be inferred from the response of the PSW system to changes in the pump parameters.

Experiments were conducted on the easy-plane antiferromagnet $MnCO_3$ at a pump frequency of $\omega_p/2\pi = 35.5\,\text{GHz}$ and at liquid-helium temperatures

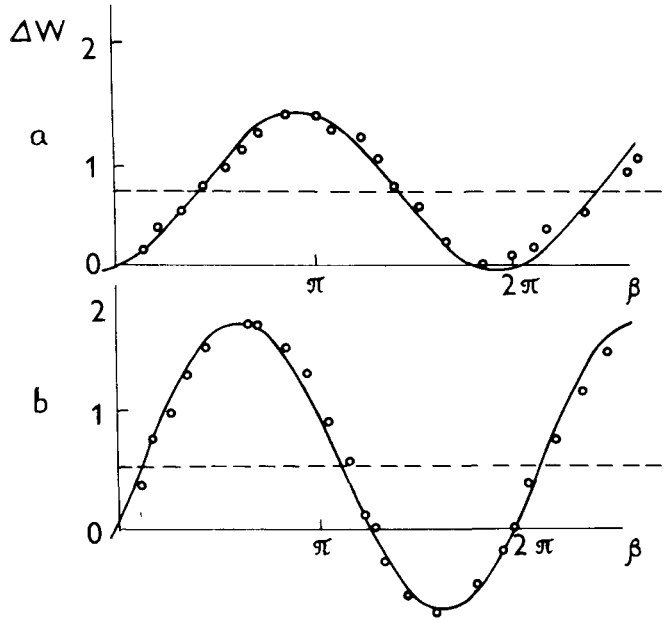

Fig. 8. Variation in power ΔW absorbed by $CsMnF_3$ versus variation of the pump phase. (a) $h/h_{th} = 1.08$; (b) $h/h_{th} = 2.25$. $T = 1.62$ K, $H = 2.55$ kOe (Prozorova and Smirnov 1974).

(Prozorova and Smirnov 1974). A rapid variation of the pump phase was implemented in the following way: a short pulse ($\tau_p \approx 0.1$ μs) was sent to the repeller plate of the klystron. During the time of the pulse the klystron generated with a frequency differing from ω_p by $\Delta\omega_p$. Thus, following this pulse, the phase of the microwave signal was shifted with respect to its initial phase by the amount $\beta \approx \Delta\omega_p\tau_p$. It was found that parametric SW respond to the change in the pump phase: depending upon β, directly after the "phase-rotating" pulse, the power absorption can be either greater or less than in the stationary state. Moreover, at definite values of β, the spin system radiates, delivering energy to the resonator. Then, during a time of approximately 1 μs, the system returns to the stationary state. The stationary phase of the standing wave formed by the PSW pair Ψ was determined from the response to the variation of the pump phase.

In fig. 8 the results of the experiment are shown: the variation ΔW of the absorbed power in the sample versus the change of the pump phase β. It follows from an analysis of these results that Ψ differs more from its optimal value (corresponding to maximum power absorption), the greater the ratio h_{th}/h. This leads to a weakening of the coupling with the pump field and, consequently, to a limitation of the PSW amplitude. The obtained experimen-

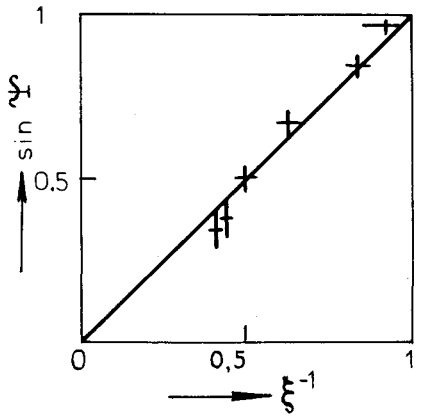

Fig. 9. Stationary phase Ψ of a pair versus supercriticality ξ^{-1}. Crosses: results of an experiment conducted on $CsMnF_3$ monocrystals at $T = 1.62$ K and $H = 2.55$ kOe. The solid straight line is the prediction of the *S*-theory with $\eta = 0$ (Prozorova and Smirnov 1974).

tal dependence $\Psi(\xi)$, plotted in fig. 9, agrees with that predicted theoretically for the phase mechanism of limitation of the amplitude. Analogous experiments were conducted on YIG (Prozorova and Smirnov 1975).

4.3. Nonlinear frequency shift and calculation of $T(\boldsymbol{k}, \boldsymbol{k}')$

The rapid variation of $n(\boldsymbol{k})$ at the moment the parametric instability is developing should lead to a mismatch between the inherent frequency of the SW and the pump frequency. This can also be noted from the appearance of a definite kind of distortion of a pulse that passes through the resonator. But the frequency renormalization cannot be investigated in such an experiment with sufficient accuracy, because the amplitude of the microwave field and the SW damping change at the moment the instability is developed.

Prozorova and Smirnov (1978) chose the following method to investigate the nonlinear frequency shift: the change of the frequency $\tilde{\omega}(\boldsymbol{k})$ of SW was measured upon a rapid change in the number of other SW, those with a frequency $\tilde{\omega}(\boldsymbol{k}')$. For this purpose, two pump signals with the frequencies $\omega_p = 2\omega(\boldsymbol{k})$ and $\omega_{p'} = 2\omega(\boldsymbol{k}')$, parametrically exciting SW of different frequencies, were applied to the crystal under investigation. The sample was placed in a rectangular resonator containing a copper strip. The dimensions of the cavity resonator were chosen so that the frequency of the mode TE_{012} of the resonator corresponded to ω_p, and the frequency of the inherent mode of the strip resonator to the lower frequency $\omega_{p'}$. The crystal was placed in the antinode of both high-frequency magnetic fields and was set up to satisfy the conditions for parallel pumping. The use of microwave filters ensured separate reception of the signals.

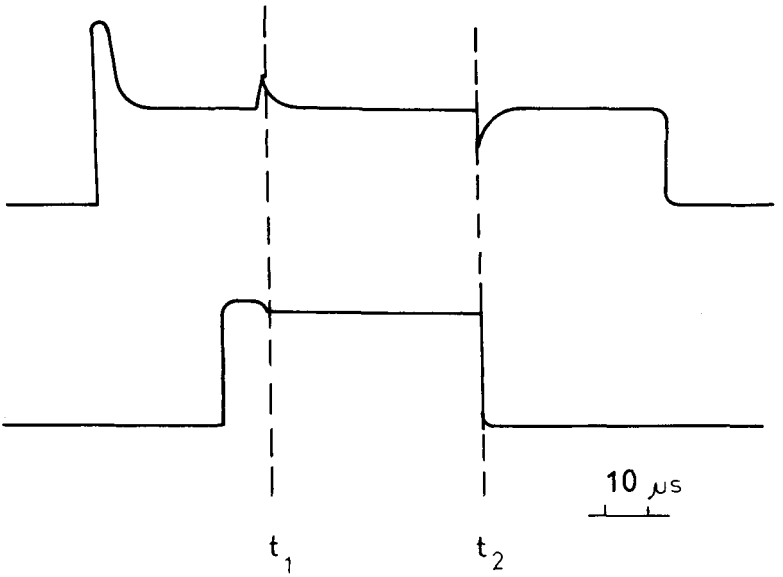

Fig. 10. Oscillogram of pulses after passing through the resonator. The lower beam ($\omega_p/2\pi = 35.1$ GHz) corresponds to the excitation of PSW1, which cause a shift of the SW spectrum; the upper beam ($\omega_{p'}/2\pi = 21.36$ GHz) corresponds to excitation of PSW2, which detects this shift (Prozorova and Smirnov 1978).

Measurements were carried out on monocrystals of $CsMnF_3$ at $T = 1.62$ K with the frequencies $\omega_p/2\pi = 21.36$ GHz and $\omega_{p'}/2\pi = 35.1$ GHz, in magnetic fields allowing parametric SW excitation at both frequencies. In fig. 10 oscillograms are shown of microwave pulses that had passed through the resonator. The upper beam corresponds to the signal with frequency ω_p, the lower beam to that with frequency $\omega_{p'}$. It can be seen that at the moment the amplitude of the SW with frequency $\omega(\boldsymbol{k}')$ (which we shall call PSW2) shows an avalanche type of increase, and also at the moment the microwave power of frequency $\omega_{p'}$ is switched off, transient processes are observed in the upper pulse. This can be interpreted as a transition of the system of PSW1, excited by the pump field with frequency ω_p, to a new stationary state, related to the renormalization of the frequency $\tilde{\omega}(\boldsymbol{k})$ due to the increase of the amplitude of PSW2. In the stationary state the conditions $\dot{\Psi}(\boldsymbol{k}) = 0$ and $\dot{n}(\boldsymbol{k}) = 0$ and eqs. (46) should be satisfied. If eqs. (46) are not satisfied, the phase $\Psi(\boldsymbol{k})$ deviates from its stationary value and, according to eq. (9), the quantity W_- changes, this being evident in the pulse that has passed through the resonator.

The nonlinear frequency shift was measured using the fact that an analogous transient process should be observed in a pulse of frequency ω_p upon a discontinuous change of the pump frequency by an amount

$$\delta\omega_p = -2\Delta,$$

because also in this case eqs. (46) are not satisfied (Prozorova and Smirnov 1974). To change ω_p, an additional rectangular pulse with a variable slope of its front edge was sent to the repeller plate of the corresponding klystron. Setting the time for the change of the pump frequency equal to the development time of the avalanche type of amplitude increase and to the SW lifetime, respectively, and selecting $\delta\omega_p$ such that the transient processes are completely identical, we can, by means of relation (67), determine the frequency shift Δ. It was established that the quantity Δ is proportional to the amplitude of PSW2. Then the coefficient $T_{kk'}$ was calculated (for a sample of $CsMnF_3$ with a volume of 1 cm^3 and placed in a field of 1.1 kOe, $T_{kk'}/2\pi \approx 3 \times 10^{-12}$ Hz). In the calculation the value of $n(\boldsymbol{k}')$ used was determined from eq. (11). The theoretical relation $T_{kk}(\boldsymbol{H})$ was calculated for an EP AFM by L'vov and Shirokov (1974). Within the limits of experimental accuracy, the experimental and theoretical results agree.

4.4. Nonlinear susceptibility

The measurement of the high-frequency susceptibility $\chi = \chi' + i\chi''$ is a traditional method of investigating the above-threshold state. The quantity χ'' determines the absorbed power,

$$W_- = \tfrac{1}{2}\chi''\omega_p h^2. \tag{68}$$

After applying eq. (9) we have

$$h\chi'' = 2\sum_k |V_k||b_k|^2 \sin[\Psi_p(\boldsymbol{k}) - \Psi(\boldsymbol{k})]. \tag{69}$$

The expression for the real part of χ can be obtained in an analogous way,

$$h\chi' = -2\sum_k |V_k||b_k|^2 \cos[\Psi_p(\boldsymbol{k}) - \Psi(\boldsymbol{k})]. \tag{70}$$

For $h < h_2$, when one group of pairs is excited, it follows from eqs. (43), (44) and (61) that

$$\chi'' = \frac{2V^2}{|S|}\left(\frac{C}{C^2+1} + \frac{(1-C^2)[\xi^2(C^2+1)-1]^{1/2} - 2C}{\xi^2(C^2+1)}\right), \tag{71}$$

$$\chi' = \frac{2V^2}{S}\left(\frac{-C + [\xi^2(C^2+1)-1]^{1/2}}{\xi^2(C^2+1)}\right)^2. \tag{72}$$

Here $C = \eta/|S|$. From this it follows that for $C \gg 1$,

$$\chi' = 0, \qquad \chi'' = 2V^2(\xi - 1)/\eta\xi. \tag{73}$$

In the opposite case, when $C \ll 1$, we obtain from eqs. (71) and (72) for the phase mechanism of limitation of the amplitude,

$$\chi' = 2V^2(\xi^2 - 1)/S\xi^2, \qquad \chi'' = 2V^2\sqrt{\xi^2 - 1}/|S|\xi^2. \tag{74}$$

It can be seen that the basic difference between the dissipative and phase mechanisms is manifest in the behavior of χ': $\chi' \ll \chi''$ for the dissipative mechanism and $\chi' \approx \chi''$ for the phase mechanism.

The susceptibility is usually measured by the change of the parameters of a high-quality resonator with the sample under investigation: χ'' is calculated from the change of the quality of the resonator, and χ' from the frequency shift. This method leads to a large error, especially for χ', because the frequency shift of the resonator does not usually exceed the half-width of its resonance curve. Application of larger samples leads to strong distortion of the resonance curve and, moreover, the error grows due to the distorted distribution of the microwave field, corresponding to the standard mode of the resonator. Additional difficulties in the measurement appear upon operation under pulsed conditions, and also because χ depends upon the amplitude of the field in the resonator. All of these factors lead to a situation in which, until recently, there existed a wide spread in the experimental data of various investigators, and there was no unambiguous interpretation of the nature of the above-threshold state.

In the investigation of the above-threshold state in YIG conducted by Melkov and Krutsenko (1977), the measuring procedures were essentially improved and the errors in the measurements were reduced to several per cent. A block diagram of their experimental setup is shown in fig. 11. The amplitude and phase of the oscillations in the resonator are measured by comparing a signal which has passed through it with a reference signal. At a pump amplitude below the threshold value ($h < h_{\mathrm{th}}$), the error signal is compensated to zero. For $h > h_{\mathrm{th}}$ a magnetization $m_z(\omega) = \chi h$ appears in the sample. This magnetization varies with the pump frequency and is directed along $\boldsymbol{H}$. The magnetization m_z sets up an additional microwave magnetic field $\tilde{h}(m_z)$ in the resonator. This leads to a change in the amplitude and phase of the total magnetic field of the resonator with respect to the amplitude and phase of the pump field. These changes can be measured by means of a phase rotator PR and a precision attenuator PA, placed in the reference signal channel, by compensating for the error signal appearing due to the excitation of PSW. Obviously, if we know the change of the amplitude $\tilde{\xi} = \tilde{h}/h_{\mathrm{th}}$ and the phase $\tilde{\varphi}$ of the field in the resonator, we can obtain information on the modified microwave magnetic field $h_{\mathrm{p}}(m_z)$ and, consequently, on the nonlinear susceptibility,

$$\chi' = -\tilde{\xi} A \sin\tilde{\varphi},$$

$$\chi'' = \tilde{\xi} A \sin\tilde{\varphi}\,(\cot\tilde{\varphi} - \sin\tilde{\varphi}/\xi), \tag{75}$$

where

$$A = 4\pi\omega_{\mathrm{p}}^2 \int_{\mathrm{sam}} h^2 \,\mathrm{d}v \Big/ \int_{\mathrm{res}} h^2 \,\mathrm{d}v.$$

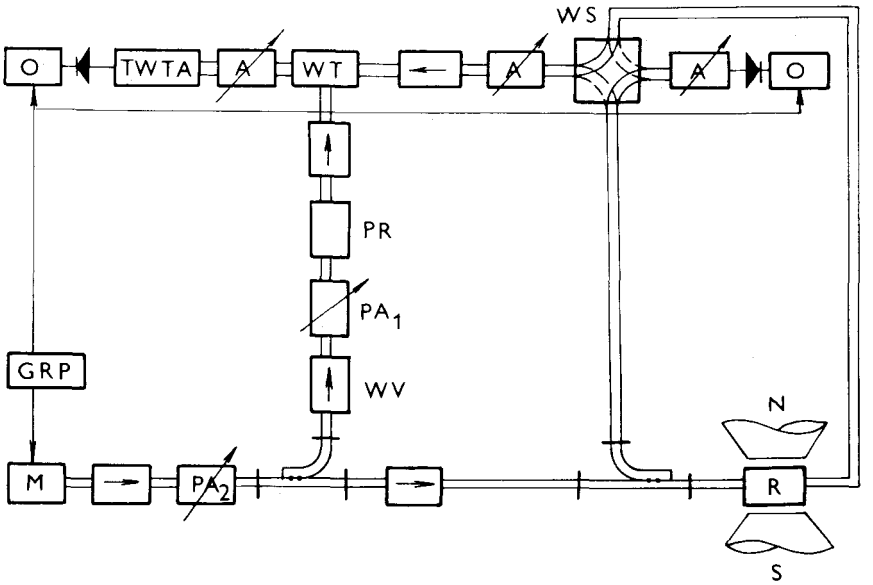

Fig. 11. Block diagram of the experimental setup for measuring the susceptibility χ (Melkov and Krutsenko 1977). M, magnetron; GRP, generator of rectangular synchronization pulses; WV, waveguide valve; WT, waveguide tee; PA, precision attenuator; PR, phase rotator; TWTA, travelling wave tube amplifier; O, oscillograph; A, attenuator; WS, waveguide switch; R, resonator.

It is clear, of course, that χ can be used to calculate the phase Ψ of the pair of waves, so that $\tan \Psi = -\chi''/\chi'$.

Measurements were made at $\omega_p/2\pi = 9.37$ GHz is pulsed operation (pulse length 200 μs and repetition frequency 50 Hz). Spheres of YIG with a diameter between 1 and 4.15 mm were investigated. The experiments were conducted at room temperature. In the paper mentioned, careful investigations of the above-threshold state in ferrite were carried out.

We cite here only a small part concerning the mechanisms of SW amplitude limitation. For $\boldsymbol{H}\|[100]$ in YIG a stationary state is established above the threshold of parametric excitation. The results of the measurements of the nonlinear susceptibility in a field $H > H_3$ are given in fig. 12. In this case there is no positive nonlinear damping. It follows from fig. 12 that there is good agreement between the experimental relation $\chi(\xi)$ and the predictions of the S-theory with $\eta = 0$. Disagreement with eqs. (74) occurs only for $\xi > 8$ dB, and is caused by the excitation of the next group of waves.

Figure 13 demonstrates the effect of positive nonlinear damping on the phase $\Psi(\boldsymbol{k})$. A careful analysis of the dependences of $\Psi(\boldsymbol{k})$, χ' and χ'' on the supercriticality at various $\boldsymbol{H}$ values enabled Melkov and Krutsenko (1977) to determine the dependence of the ratio $\eta/|S|$ on the magnetic field. This

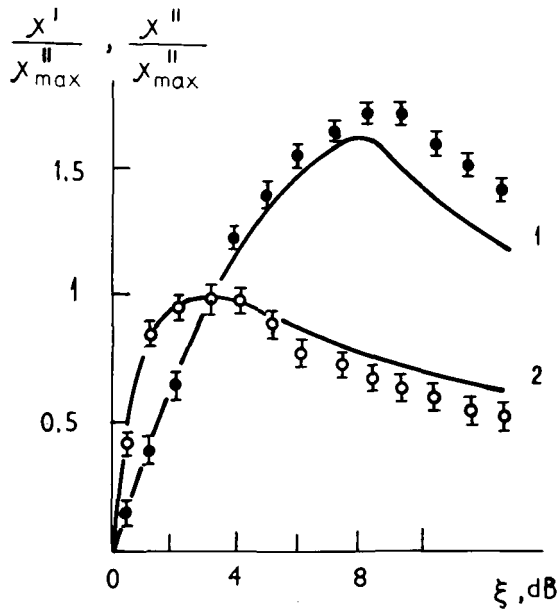

Fig. 12. Susceptibility in parallel pumping of PSW versus supercriticality (Melkov and Krutsenko 1977). Measurements were made on a YIG sphere 2 mm in diameter at $\boldsymbol{H}\|[100]$. $H = H_c - 50\,\text{Oe}$ ($k \approx 0$ at $H = H_c$). Solid lines represent theoretical calculations: χ', curve 1; χ'', curve 2.

dependence is in good agreement with the theoretical dependence shown in fig. 5.

The following results were obtained for the above-threshold susceptibility in an easy-plane AFM. In $CsMnF_3$ and $MnCO_3$ the behavior of $\chi(\xi)$ agrees with the S-theory with $\eta = 0$ (Kveder and Prozorova 1974). In $FeBO_3$, in which at low temperatures the main SW relaxation mechanism is the three-particle magnon–phonon decay process and therefore positive nonlinear damping is high, $\chi' = 0$ within the experimental accuracy (Kotyuzhansky and Prozorova (1984).

4.5. Electromagnetic radiation by parametrically excited spin waves

The investigation of PSW radiation is of interest, first of all, because it enables one to determine the spectral composition of PSW, i.e. the quantity $N(\omega)$ (see eq. (59)]. It should be mentioned that direct electromagnetic radiation of PSW with $k \approx 10^4$ to $10^6\,\text{cm}^{-1}$ is extremely weak due to the momentum conservation law $k_p \ll k$. Nevertheless, with the application of up-to-date microwave techniques such investigations could be carried out recently.

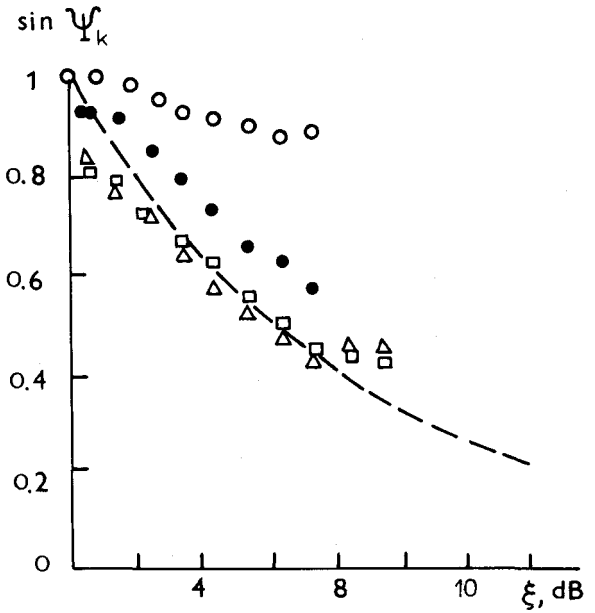

Fig. 13. Dependence of the phase Ψ of the pair of waves on the supercritically at various values of the magnetic field: (△) $H = H_c - 500$ Oe; (□) $H = H_c - 600$ Oe; (●) $H = H_c - 550$ Oe $= H_{3m}$; (○) $H = H_c - 1000$ Oe $< H_3$ (if $H = H_c$ then $k \approx 0$). Simple: YIG sphere, 2 mm in diameter, $\boldsymbol{H} \| [100]$. The dashed curve is the relation $\sin \Psi(\xi)$, calculated by the S-theory in the absence of nonlinear damping ($\eta = 0$) (Melkov and Krutsenko 1977).

4.5.1. Frequency of spin waves excited by parallel pumping

It follows from the conservation laws of eq. (1) that SW are parametrically excited at a frequency equal to one-half the pump frequency. An important question remains the accuracy with which condition (1) is satisfied in an experiment. Are magnons excited only with a frequency $\omega(\boldsymbol{k})$ exactly equal to $\omega_p/2$, so that the spectral distribution $n[\omega(\boldsymbol{k})]$ has the form of a δ-function, or does excitation take place in a certain frequency band $\delta\omega(\boldsymbol{k})$? The fact that the excited magnons have a frequency $\omega(\boldsymbol{k}) = \omega_p/2$ can be established with low accuracy from the region of existence of additional absorption, as well as from experiments in which singularities are observed in the PSW relaxation at the point of intersection of the magnon and (known from other experiments) phonon spectra (Turner 1960, Seavey 1969b, Kveder et al. 1972). A more accurate determination of the frequency of PSW with $k \approx 10^4$ to 10^6 cm^{-1} was achieved in experiments on Mandelstam–Brillouin scattering of light by PSW (Venitsky et al. 1978, Zhotikov and Kreines 1979). But the error in the determination of the frequency of magnons in optical experiments (1 GHz) is still too large for a measurement of $\delta\omega(\boldsymbol{k})$.

The most direct and accurate method to determine the spectral distribution of PSW can be a study of the spectral composition of the radiation $I(\omega)$ caused by the PSW. We can readily estimate the spectral density $I(\omega)$ of the radiated energy,

$$I(\omega) = 8\omega^4(\boldsymbol{k})M|\Delta M|N(\omega)/3C^3k^2V^{2/3}, \tag{76}$$

where ΔM is the change of the magnetization when one SW is excited. Of interest is the fact that in AFM with weak ferromagnetism ($H_D \neq 0$), the quantity ΔM can substantially exceed the Bohr magneton μ_B. As a matter of fact

$$\Delta M = -\hbar \frac{\partial\omega(\boldsymbol{k})}{\partial H} = -\frac{g(H + H_D)}{2\omega(\boldsymbol{k})}\mu_B. \tag{77}$$

Hence, it is clear from eqs. (76) and (77) that in order to observe radiation it proves expedient to increase the pump frequency and to use a substance with a high H_D value.

PSW radiation was investigated by Kotyuzhansky et al. (1983, 1984). Monocrystals of $FeBO_3$ were used (the samples were cylinders, 2 mm in diameter and 3 mm high). The axis of the cylinders was along the principal axis of the crystal. Microwave pumping was provided by a continuous magnetron oscillator with a frequency $\omega_p/2\pi = 35.6$ GHz and a power of 10 W. The cylindrical resonator of the microwave spectrometer was adjusted so that the frequency of its TE_{012} mode coincided with ω_p. The sample was mounted in the exit coupling window of the resonator, symmetrically positioned with respect to its wall, which is 0.5 mm thick. Thus, one part of the sample was located inside the resonator at the antinode of the microwave magnetic field $\boldsymbol{h}$, and the other part in a standard waveguide in the 1.5 cm microwave range. The fields $\boldsymbol{h}$ and $\boldsymbol{H}$ were in the basal plane of the crystal and parallel to each other. By means of microwave filters the output signals with frequencies ω_p and $\omega_p/2$ were separated from each other. The decoupling between the channels was 40 dB. The signal at the frequency $\omega_p/2$ was fed to a superheterodyne receiver with a sensitivity of 10^{-14} W and analyzed by means of a spectrum analyzer.

It was established in the experiments that, above the threshold of parametric excitation, radiation from the sample at the frequency $\omega_p/2$ appears simultaneously with the absorption of microwave pump power at the frequency ω_p. The radiation intensity $I(\omega)$ depended upon time in a random manner. The oscillogram of the receiver output signal had the form of spikes with a characteristic duration $\tau \sim 10^{-5}$–10^{-6} s. A fundamentally important result of the experiment was the fact that the center of the radiation band coincided with $\omega_p/2$ with an accuracy of $\pm 2\pi \cdot 20$ kHz, i.e. with a relative accuracy of the order of 10^{-6}. This was established by applying to the receiver input, simultaneously with the radiation signal, a signal from a supplementary klystron

microwave oscillator, tuned so that its second harmonic coincided with the pump frequency. The klystron was finely tuned to secure zero beat between the klystron and magnetron signals. Within the measurement error of the frequency associated with parasitic deviations of the klystron and magnetron frequencies, the frequencies of the klystron and radiation coincided.

4.5.2. Frequency width of a parametrically excited spin wave packet

(a) *PSW amplitude limitation by nonlinear damping in the easy-plane antiferromagnet $FeBO_3$.* A previously cited paper (Kotyuzhansky et al. 1984) also discusses the shape of the wave packet, $N(\omega)$. It was found that the width of the wave packet, $\Delta\omega$, increases linearly with supercriticality ξ (see fig. 14). The broadening of the radiation line, $N(\omega)$, in $FeBO_3$ was investigated theoretically by Mikhailov and Chubukov (1984). The theoretical estimate of the linewidth, $\Delta\omega$, obtained in this paper is less than the experimentally observed value by a factor of 25. The form of the dependence of $\Delta\omega$ on ξ obtained by Mikhailov and Chubukov (1984) [see eq. (64)] coincides with the experimental data only for $\xi > 4$. This disagreement is evidently due to certain simplifications in the theory (Mikhailov and Chubukov 1984), in particular, the assumption of equilibrium of the phonons. As shown by L'vov (1975), the shape of the wave packet, $N(\omega)$, is not associated with any specific mechanism of nonlinear damping and is determined in accordance with eq. (50) by the general structure of the Green's function (49). Mikhailov and Chubukov (1984) showed (see fig. 15) that the experimentally observed line shape $N(\omega)$ coincides with the theoretical data (L'vov 1975).

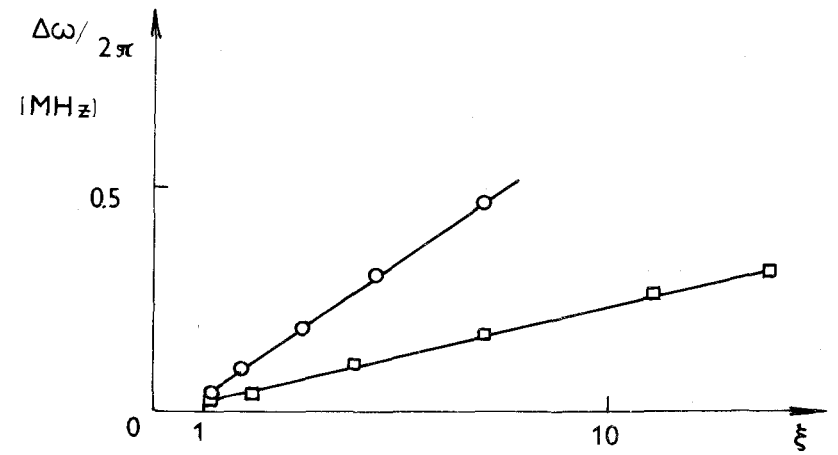

Fig. 14. PSW radiation linewidth in $FeBO_3$ versus pump amplitude for $H = 380$ Oe. (Width was measured at the level $0.1\,I_{max}$.) (□) $T = 1.2$ K; (○) $T = 4.2$ K (Kotyuzhansky et al. 1983).

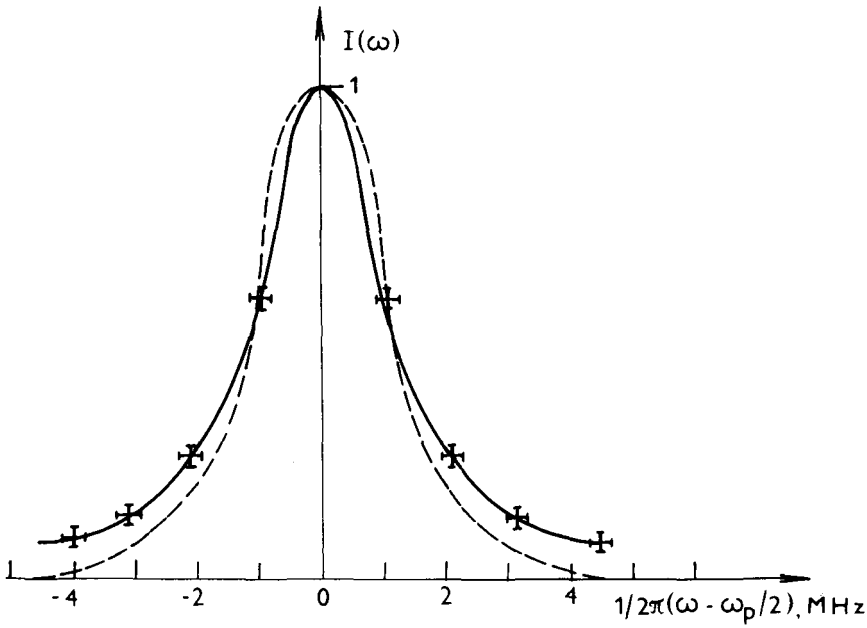

Fig. 15. PSW radiation lineshape in $FeBO_3$. The solid line is the theoretical relation calculated from equations given by L'vov (1975) and Mikhailov and Chubukov (1984), in which the half-width is taken equal to the experimentally observed value (Kotyuzhansky et al. 1984); the dashed line is a Lorentzian of the same width.

(b) *PSW amplitude limitation by the phase mechanism in the ferromagnet YIG.* Krutsenko et al. (1978) applied another procedure to investigate the shape of the wave packet, $N(\omega)$, in YIG. The samples used in their experiments were ferrite spheres made of YIG monocrystals, 2.5 to 2.9 mm in diameter. They were at room temperature. The pump frequency $\omega_p/2\pi = 9.37$ GHz. The spheres were oriented with the hard direction of magnetization $[100] \| \boldsymbol{H}$ to exclude the effect of low-frequency self-oscillations of the magnetization. The electromagnetic radiation from the ferrite is maximal when the frequency of this radiation is equal to the natural frequency of one of the magnetostatic modes. The registering circuit consisted of a 6 cm range amplifier, protected against the pump frequency by a low-frequency filter, a square-law detector and a spectrum analyzer of single-frequency range.

The experiment showed that, in contrast to $FeBO_3$, the linewidth $N(\omega)$ of excited spin waves is of the order of several kilohertz (in the damping of SW, γ is equal to several hundred kilohertz). The experimental dependences of $\Delta\omega$ on H, k and ξ are satisfactorily described by the S, T^2-theory discussed in section 3.6. In particular, the lineshape $N(\omega)$ is close to an inverse hyperbolic cosine [in accordance with eq. (59)] and cannot be approximated by Lorentzian and Gaussian curves.

5. *Nonstationary processes in parametric excitation of spin waves*

5.1. *Spectrum of collective oscillations*

Here we shall discuss the behavior of a PSW system upon a small deviation from the stationary state. For simplicity we shall restrict ourselves to fields h up to the second threshold, when only one group of pairs of waves is excited in the ground state. Linearizing the equation of motion (28) with respect to the ground state $n(\boldsymbol{k},t) = n_{st}(\boldsymbol{k})$ [see eq. (41)] and assuming

$$\delta n(\boldsymbol{k},t) = [n(\boldsymbol{k},t) - n_{st}(\boldsymbol{k})] \propto \exp(i\Omega t),$$
$$\delta\Psi(\boldsymbol{k},t) = [\Psi(\boldsymbol{k},t) - \Psi_{st}(\boldsymbol{k})] \propto \exp(i\Omega t), \tag{78}$$

we can obtain a system of equations, homogeneous with respect to δn and $\delta\Psi$, that describe the free collective oscillations (CO) in the PSW system with respect to the ground state. The condition for the solvability of these equations is determined by the complex frequency Ω_m of the CO:

$$\Omega_m^{\pm} = -i\gamma \pm [\Delta_m^2 - \gamma^2]^{1/2}, \quad \Delta_m = 4S_m(2T_m + S_m)N_1^2. \tag{79}$$

In the case of AFM, when the parametric excitation of SW is spherically symmetric, m is the number of the spherical harmonic, characterizing the angular dependence of the excitations $\delta n(\boldsymbol{k},t)$ and $\delta\Psi(\boldsymbol{k},t)$. In the case of FM, when the PSW are excited axially symmetrically on the equator of the resonance surface, the index m is the number of the axial harmonic,

$$\delta n(\boldsymbol{k},t) \propto \exp(im\varphi), \qquad \delta\Psi(\boldsymbol{k},t) \propto \exp(im\varphi). \tag{80}$$

From eq. (79) the important conclusion follows that $\operatorname{Im}\Omega_m^{+} > 0$ when

$$S_m(2T_m + S_m) < 0. \tag{81}$$

In this case the amplitude of the CO [see eq. (78)] will grow exponentially with time, and this indicates the instability of the ground state. The nonlinear stage of development of this instability, spontaneous self-oscillations, shall be described in section 5.3 and 5.4. We shall begin by assuming that

$$S_m(2T_m + S_m) > 0, \tag{82}$$

and that the ground state is stable. In conclusion we note that within the scope of the S-theory, CO systems of PSW are spatially uniform. When spatial dispersion is taken into account, each normal mode corresponds to a whole branch $\Omega_m((\kappa)$, and its gap is determined by eq. (79). Spatially nonuniform CO, with $\delta n \propto \exp[i(\kappa\cdot\boldsymbol{r} - \Omega_m t)]$ and $\delta\Psi \propto \exp[i(\kappa\cdot\boldsymbol{r} - \Omega_m t)]$ are in a definite sense analogous to second sound waves. In contrast to ordinary second sound in a gas of thermal magnons, not only does the number n_k of pairs of waves vary in a PSW system, but their phase Ψ_k as well.

5.2. Resonant excitation of collective oscillations. Theory and experimental investigation

The above-discussed CO system of PSW can be excited (like oscillations of any other nature) in various ways: with the aid of external resonance, parametrically or by impact. All these methods of CO excitation have been used in experiments performed on ferro- and anitferromagnets.

It is simplest to devise a theory and to interpret experiments for the resonance method of CO excitation. This, exactly, is the way they were discovered by Zautkin, et al. (1972a). In addition to parallel pumping (at a frequency $\omega_p/2\pi \approx 10\,\text{GHz}$) they applied to the YIG sample another microwave signal of the same polarization, whose frequency ω_s differed from ω_p by the frequency of the CO. Calculations carried out by Zautkin et al. (1972a) by means of the equations of motion (28) of the S-theory indicate that for a weak signal the dependence of the susceptibility on its frequency ω_s should have two singularities of a resonance type. The frequency of these peaks should be at a distance $\pm\Delta_0$ from ω_p, where Δ_0 is determined by expression (79),

$$\Delta_0^2 = 4S_0(2T_0 + S_0)N_1^2 = 4\gamma^2(\xi^2 - 1)(2T_0 + S_0)/S_0. \tag{83}$$

For $\xi > 2$, when $\Delta_0 > \gamma$, the lineshape is close to a Lorentzian, with a width equal to the damping γ of the SW. At the resonance points, the imaginary part of the susceptibility χ_s'' is given by

$$\chi_s''(\omega_p \pm \Delta_0) = \xi^2\left[1 \pm \left(1 + \frac{T_0^2}{S_0(2T_0 + S_0)}\right)^{1/2}\right]\frac{V^2}{|S|}. \tag{84}$$

It is of importance in principle that the susceptibility may become negative. This does not correspond to absorption, but to the amplification of a weak signal. It follows from eq. (84) that absorption takes place at the frequency $\omega_p + \Delta_0$, and amplification at the mirror frequency $\omega_p - \Delta_0$.

The origin of the amplification can be seen as a result of instability of the ground state (with "slow" frequency equal to zero) to decay into electromagnetic radiation (with "slow" frequency Ω) and a collective oscillation at the natural frequency Δ_0. The energy conservation law in this process is $0 \to \Omega + \Delta_0$. This amplification takes place at the frequency $\Omega = -\Delta_0$, which corresponds to eq. (84). The observed absorption is a result of the decay of a weak signal into the ground state and CO with the conservation law $\Omega = 0 + \Delta_0$.

The experimental results obtained by Zautkin et al. (1972a) agree well with the theoretical data. In particular, the measured relation $\chi_s''(\xi^2)$ is linear to a good accuracy, in accordance with eq. (84). The dependence of Δ_0 on ξ^2 also agrees with the theory: eq. (83) and fig. 16.

The above-discussed method of generating CO at the frequency Ω by means of a longitudinal microwave field h_z at the frequency $\omega_p + \Omega$ is somewhat

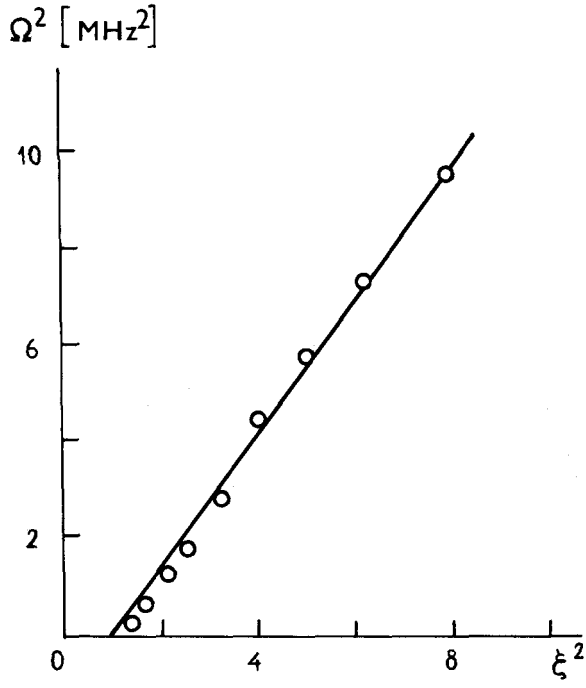

Fig. 16. Dependence of the frequency Ω of CO on the pump power (Zautkin et al. 1972a).

artificial. It would seem more natural to use a RF magnetic field at the frequency Ω. But the first attempts to register this effect were not successful because of the low susceptibility in the RF range. It was only in 1975 that Orel and Starobinets (1975) succeeded in observing this effect by means of a highly sensitive procedure.

A theory was developed by Zautkin et al. (1977) and data were obtained for the experimental observation of the parametric excitation of CO in a system of parametrically excited SW. The authors called this phenomenon double parametric resonance. The SW were pumped by a microwave field h with frequency ω_p. The CO were pumped by a RF field h_z, parallel to the CO, with frequency Ω. Above a certain critical value (threshold $h_z = h_{zc}$) radiation at the frequency $\Omega/2$ appeared. The theoretically calculated and experimental dependences of h_{zc} on H agree well with each other.

Closely related to the resonance methods of exciting CO is the method of impact excitation of CO by means of a drastic change in the pump phase. This method was realized by Prozorova and Smirnov (1974). Their data on the natural frequency of CO in the antiferromagnet $MnCO_3$ also agree well with the theoretical dependence, eq. (83).

5.3. *Properties and nature of self-oscillations of parametrically excited spin waves*

It is well known that in the parametric generation of SW the steady-state condition is often not established, and the magnetization carries out complex self-oscillations (SO) about a certain average value. The basic experimental facts concerning SO in parallel pumping are the following (Monosov 1971, Courtney and Claricoats 1964).

1. The frequency of SO lies in the range from 10^4 to approximately 10^6 Hz (depending upon the quantities ξ and H). When only slightly above the threshold, the SO spectrum consists of a single line; with increasing power level, the number of lines increases and they are shifted toward higher frequencies. In particular, components appear at multiple frequencies and at half the frequency (Monosov 1971, Grankin et al. 1981). Far above the threshold, the spectrum is noise-like.

2. The SO threshold is usually above the threshold of parametric excitation of SW by 0.1 to 1 dB, with the exception of a region of small k-values, $k \approx 10^3 - 10^4\,\mathrm{cm}^{-1}$, where the SO threshold is appreciably higher. The threshold is also increased by introducing internal defects into the crystal (Monosov 1971).

3. A strong crystallographic anisotropy of the properties of SO is observed; it considerably exceeds the anisotropy of the SW spectrum. Thus, the intensity of SO in YIG when the magnetization is oriented along the [111] axis exceeds the intensity of these oscillations along the [100] axis by approximately a factor of 100.

The problem of the physical origin of SO is one of the basic questions in the parametric excitation of SW. Various hypotheses were proposed to explain the nature of SO. The simplest hypothesis (Wang et al. 1968, Wang and Ta-Lin Hsu 1970) consists in the assumption that in the PSW spectrum there are certain discrete frequencies and that the beats between them, corresponding to the natural oscillations of the crystal, lead to the appearance of SO. This hypothesis explains a number of experimentally observed facts (dependence of the frequency of SO on the magnitude and direction of the magnetic field), but completely ignores the question of the dependence of the SO frequency on the pump power and, in general, the problem of the origin of several discrete frequencies. We point out that the S-theory predicts the existence in the stationary state of only the frequency $\omega_p/2$.

Another group of hypotheses is associated with the effect of PSW on the magnetization [see, for example, Green and Schlömann (1968)]. If the average magnetization of the crystal follows the amplitude of SW with a certain lag, SO of the magnetization can be built up in such a crystal. The monograph of Monosov (1971) is written from this point of view, based on the phenomenological Bloch–Bloembergen equation. Actually, however, the appearance of SO can be affected only by the inertia of thermal SW with a frequency of the

order of ω_p. Therefore, the problem of the effect of the inertia of thermal SW should be solved by means of a kinetic equation. It can be assumed that in the majority of experimental situations the effect of inertia can be neglected.

Within the scope of the *S*-theory, self-oscillations have a natural explanation as a result of the instability of the stationary state with respect to the excitation of CO, as described in section 5.1. If the instability condition (81) is satisfied even for a single mode with number m, then, within the framework of the *S*-theory, the PSW system has no stable stationary states. In this case there are two conceivable possibilities: "the system is driven beyond the limits of applicability of the *S*-theory (in which case the amplitude of the excited waves must drastically increase) or an oscillation about the stationary state is established. In an experiment these oscillations are observed as SO of the magnetization. From general considerations, it should be expected that self-oscillations, in general, may be either regular or chaotic.

5.4. Transition from periodic to chaotic conditions of self-oscillations: a laboratory and a numerical experiment

As can be seen from eq. (79), the instability of the stationary state is purely aperiodic ($\mathrm{Re}\,\Omega_m = 0$). This makes an analytic solution of the problem of the nonlinear stage of its development extremely difficult. Therefore, numerical simulation proves to be expedient. In this case, the calculation of a real situation, for example, for YIG, would require a huge amount of computer time and would hardly be feasible. This made it necessary to resort to a numerical experiment on simplified models of the ground state.

L'vov et al. (1973) and Grankin et al. (1981) describe a numerical experiment for the excitation of SO on a "two-beam" model in which it was assumed that the SW are concentrated at two fixed angles $\vartheta_1 = \pi/2$ and $\vartheta_2 = \pi/4$. The

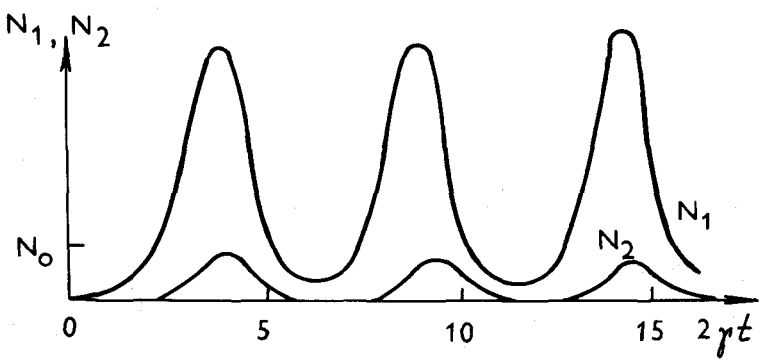

Fig. 17. Time dependence of the amplitude of pairs of waves on beams at the instability of the zero ($m = 0$) mode. N_1 and N_2 correspond to the beams $\vartheta = \pi/2$ and $\vartheta = \pi/4$ (L'vov et al. 1973).

values of the coefficients $S(\boldsymbol{k}, \boldsymbol{k}')$ and $T(\boldsymbol{k}, \boldsymbol{k}')$ were chosen close to those calculated for YIG at the orientation $\boldsymbol{H} \| [111]$ (see below), so that the condition for instability of a mode with $m = 0$ was satisfied. The numerical experiment showed that in such a model there are SO of the amplitudes N_1 and N_2 and wave phases Ψ_1 and Ψ_2 of the beams (fig. 17). The dependence of the frequency of these SO on the pump level agrees qualitatively with an analogous dependence usually observed in a laboratory experiment.

Another experiment was performed with the two-beam model in which the development of a collective instability for $m \neq 0$ was simulated. In this experiment the behavior of the numbers of SW, N_1 and N_2, in the nonlinear stage of development of the instability were also investigated. This is of interest because in the linear stage no change occurs in the sum $N_1 + N_2$. Beams were chosen with $\vartheta_1 = \vartheta_2 = \pi/2$ and $\varphi_2 = \varphi_1 + \pi/2$. The experiment showed (fig. 18) the establishment of conditions in which both the difference, $N_1 - N_2$, and the sum, $N_1 + N_2$, oscillate. The oscillations of $N_1 + N_2$ are generated due to the interaction of collective modes with different m values.

An essential result of these numerical experiments was the proof that for $\xi < \xi_c \approx 3$–4, the trajectory of the PSW system in phase space goes to a stable limit cycle, whose region of attraction is all of phase space. For $\xi > \xi_c$ trajectories close to this cycle become exponentially unstable, with the time derivative of the distance to the limit cycle increasing proportionally to $\xi - \xi_c$. For low values of $\xi - \xi_c$, a narrow layer filled with exponentially unstable trajectories is formed near the limit cycle.

The divergence of the trajectories was also investigated in a laboratory experiment (Grankin et al. 1981). For this purpose, the time evolution of $\chi''(t)$ for various pump pulses of a single series with fixed supercriticality and other conditions of the experiment were registered on one and the same screen. Due

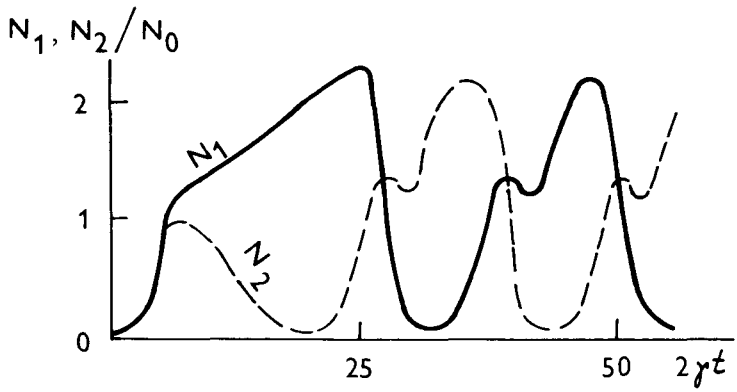

Fig. 18. Time dependence of the total amplitude of pairs of waves on beams at the instability of the mode $m = 2$ (Grankin et al. 1981).

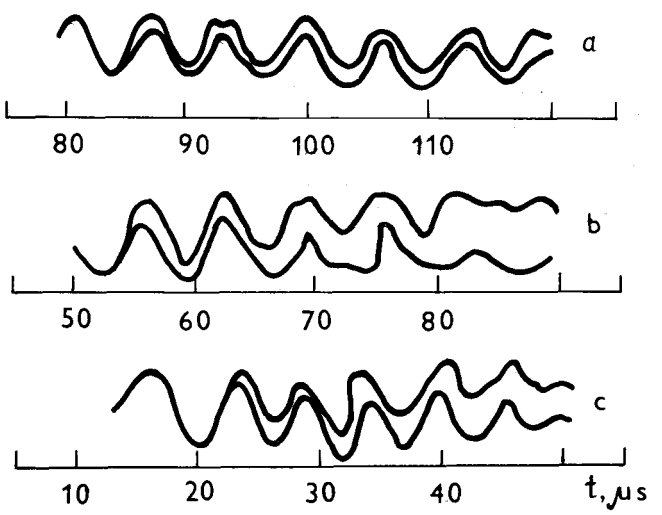

Fig. 19. Divergence of the trajectories $\chi''(t)$ in an experiment by Grankin et al. (1981). (a) $\xi^2 = 2.6$ dB; (b) $\xi^2 = 2.9$ dB; (c) $\xi^2 = 3.4$ dB.

to the fluctuations of the wave system, for different pulses we start each time with different initial conditions. At supercriticalities $\xi = 2.5$ dB, successive $\chi''(t)$ curves repeat one another. When $\xi > 2.5$ dB, the SO Fourier spectrum is drastically broadened; the $\chi''(t)$ curves for the various pulses begin to diverge. First the divergence of nearby trajectories becomes manifest only after a long time (see fig. 19). Then, as the supercriticality increases, the "divergence time" becomes comparable to the SO period: $\tau \approx (3\text{–}5)\Delta_0$ and the consecutive $\chi''(t)$ curves form a wide band (fig.19).

Summarizing, it can be said that the numerical model experiments indicate that within the framework of the *S*-theory, the development of an instability of the ground state leads to self-oscillations. The properties of these SO—dependence of the frequency and spectral composition on the pump power—resemble the properties of real SO observed in a laboratory experiment. In particular, at low supercriticalities, the SO are periodic in a laboratory and a numerical experiment. A representation of such a motion in phase space is the stable limit cycle. In both types of experiment, there is a transition to stochastic SO with increasing supercriticality. This transition is not caused by the addition of new types of motion at incommensurable frequencies, but is accompanied by a broadening of the existing spectral lines and is associated with the loss of stability of the phase trajectories, leading to their divergence. This means that secondary turbulence of SW occurs in accordance with the concept of a strange attractor.

Further, in both the numerical and the laboratory experiment, the develop-

ment of SO has no appreciable effect on the mean level of PSW. The numerical experiment indicates, besides, that in the development of the instability of the zero mode ($m = 0$), intense oscillations are set up, whereas in the development of the instability of higher modes, the oscillations have weak variations of the total number N of SW and of the quantity $\chi''(t)$. An interesting fact is that the appearance of SO in the numerical experiment was accompanied, as a rule, by a reduction of the average value of χ'. This regularity was also observed in the laboratory experiment.

In recent years, in connection with the progress of the theory of dynamic systems in investigating the transition to turbulence within the scope of the concept of the stochastic (or strange) attractor, it has again become of interest to investigate the properties of SO in a PSW system. Gibson and Jeffries (1984) have studied in detail the transition from periodic SO to chaos in YIG (with an admixture of gallium) upon parametric excitation of SW by transverse pumping at a frequency $\omega_p/2\pi = 1.3\,\text{GHz}$. The phase portrait of the SO and the return maps of the SO as functions of supercriticality were investigated. Doubling of the SO period was observed. It was shown that in the phase space of this system there are several complex attractors, with the transition between them accompanied by hysteresis.

Doubling of the SO cycle was also observed by Yamazaki (1984) in parallel pumping of SW in the AFM $CuCl_2 \cdot 2H_2O$ at a frequency $\omega_p/2\pi = 8.9\,\text{GHz}$ at a temperature 1.4 K and supercriticality $\xi \geqslant 10$. Subsequently, similar results were obtained in parametric excitation of SW by parallel pumping in the quasi-two-dimensional ferromagnet $(CH_3NH_3)_2 \cdot CuCl_4$ (Yamazaki et al. 1984). Numerical simulation of the transition to chaos of SO in models with a small number of equations was performed by Astashkina and Mikhailov (1980) and Waldner et al. (1984). The question as to whether these models conform to the experimental conditions in which SW were excited in a wide region of k-space still remains unanswered.

5.5. *Conditions for the onset of self-oscillations*

The results obtained above enable us to predict in which cases SO should be observed in real experiments.

For this purpose it is necessary to calculate the coefficients S_m and T_m and to find out which of the inequalities (81) or (82) are satisfied within the given conditions of the experiment. For YIG this program, together with the experimental investigation of SO, was carried out by L'vov et al. (1973), and subsequently in much greater detail by Zautkin and Starobinets (1974). After varying the coefficients S_m and T_m of the Hamiltonian (changing the magnetization by means of the temperature and concentration of impurities, changing the shape of the sample: sphere, cylinder and disk, and the direction of magnetization), they showed, in particular, that intense SO are formed only at

instability of the zero mode with respect to criterion (81), whereas the instability of modes with $m \neq 0$ is always accompanied by the formation of SO of small amplitude.

It is necessary to mention in conclusion that the simple theory of SO described in this section predicts that the threshold h_a of their formation coincides with the threshold h_{th} of parametric excitation, and that the frequency of SO at $h = h_a$ equals zero. In the experiments, however, a finite threshold of SO and nonzero initial frequency is observed. In YIG monocrystals, the self-oscillation threshold is usually equal to 0.1 to 1 dB, and the initial frequency does not correlate with the magnitude of the threshold; it varies, depending upon the static magnetic field, within the range from 10^4 to 10^5 Hz (Wang and Ta-Lin Hsu 1970). These facts can be explained by the effect of a weak nonlinear damping that does not appreciably change the quantities χ' and χ'', by the presence of random inhomogeneities in the crystals, by the lack of precise axial symmetry, by the reverse effect of the sample on the resonator, etc. To clarify the relative contributions of these mechanisms, further theoretical and experimental investigation of self-oscillations is required.

6. *Conclusion*

The results of the experiments and the theoretical considerations dealt with in this review indicate that considerable progress has been achieved in the understanding of the phenomena that take place in magnetic dielectrics upon parametric excitation of spin waves. The physical concepts arrived at in the study of these phenomena are applicable to many related problems. In particular, they are applicable to certain problems in plasma physics; they can also find use in investigation of the parametric excitation of waves on the surfaces of liquids, surface spin waves in magnetic films, sound in dielectrics, etc. We hope that the theory developed represents the main features of wave turbulence, set up in an unstable continuous medium at not too high supercriticality.

References

Adrienko, A.V., and L.A. Prozorova, 1985, Zh. Eksp. & Teor. Fiz. **88**, 231.
Anisimov, A.N., and A.G. Gurevich, 1975, Zh. Eksp. & Teor. Fiz. **68**, 677.
Anisimov, A.N., and A.G. Gurevich, 1976, Fiz. Tverd. Tela **18**, 38.
Astashkina, E.V., and A.S. Mikhailov, 1980, Zh. Eksp. & Teor. Fiz. **78**, 1636.
Bloembergen, N., and R. Damon, 1952, Phys. Rev. **85**, 699.
Bloembergen, N., and S. Wang, 1954, Phys. Rev. **93**, 72.
Borovik-Romanov, A.S., 1958, Zh. Eksp. & Teor. Fiz. **36**, 766.
Courtney, W.E., and P.I. Claricoats, 1964, J. Electron. Control **16** (1), 1.

Douglass, R., 1960, Phys. Rev. **120**, 1612.
Dzyaloshinsky, I.E., 1957, Zh. Eksp. & Teor. Fiz. **32**, 1547.
Gibson, G., and C. Jeffries, 1984, Phys. Rev. A **29**, 811.
Gottlieb, P., and H. Suhl, 1962, J. Appl. Phys. **33**, 1508.
Grankin, V.L., G.A. Melkov and S.M. Ryabchenko, 1975, Fiz. Tverd. Tela **17**, 358.
Grankin, V.L., V.S. L'vov, V.I. Motorin and S.L. Moosher, 1981, Zh. Eksp. & Teor. Fiz. **81**, 757.
Green, J.J., and E. Schlömann, 1968, Appl. Phys. Lett. **33**, 1358.
Hartwick, T.S., E.R. Peressini and M.T. Weiss, 1961, J. Appl. Phys. **32**, 223.
Jantz, W., J. Schneider and B. Andlauer, 1972, Solid State Commun. **10**, 937.
Kasuya, T., and R. Le Craw, 1961, Phys. Rev. Lett. **6**, 223.
Kolokolov, I.V., V.S. L'vov and V.B. Cherepanov, 1983, Zh. Eksp. & Teor. Fiz. **84**, 1043.
Kolokolov, I.V., V.S. L'vov and V.B. Cherepanov, 1984, Zh. Eksp. & Teor. Fiz. **86**, 1946.
Kotyuzhansky, B.Ya., and L.A. Prozorova, 1971, Zh. Eksp. & Teor. Fiz. Pis'ma **13**, 430.
Kotyuzhansky, B.Ya., and L.A. Prozorova, 1972, Zh. Eksp. & Teor. Fiz. **62**, 2199.
Kotyuzhansky, B.Ya., and L.A. Prozorova, 1973, Zh. Eksp. & Teor. Fiz. **65**, 2470.
Kotyuzhansky, B.Ya., and L.A. Prozorova, 1980, Zh. Eksp. & Teor. Fiz. Pis'ma **32**, 254.
Kotyuzhansky, B.Ya., and L.A. Prozorova, 1981, Zh. Eksp. & Teor. Fiz. **81**, 1913.
Kotyuzhansky, B.Ya., and L.A. Prozorova, 1984, Zh. Eksp. & Teor. Fiz. **86**, 658.
Kotyuzhansky, B.Ya., L.A. Prozorova and L.E. Svistov, 1983, Zh. Eksp. & Teor. Fiz. Pis'ma **37**, 586.
Kotyuzhansky, B.Ya., L.A. Prozorova and L.E. Svistov, 1984, Zh. Eksp. & Teor. Fiz. **83**, 1101.
Krutsenko, I.V., V.S. L'vov and G.A. Melkov, 1978, Zh. Eksp. & Teor. Fiz. **75**, 1114.
Kveder, V.V., and L.A. Prozorova, 1974, Zh. Eksp. & Teor. Fiz. Pis'ma **67**, 1952.
Kveder, V.V., B.Ya. Kotyuzhansky and L.A. Prozorova, 1972, Zh. Eksp. & Teor. Fiz. **63**, 2205.
Le Gall, H., B. Lemaire and D. Sere, 1967, Solid State Commun. **5**, 919.
Lutovinov, V.S., 1978, Fiz. Tverd. Tela **20**, 1807.
Lutovinov, V.S., and M.A. Savchenko, 1977, Zh. Eksp. & Teor. Fiz. Pis'ma **26**, 683.
L'vov, V.S., 1975, Zh. Eksp. & Teor. Fiz. **69**, 2079.
L'vov, V.S., and G.E. Fal'kovich, 1982, Zh. Eksp. & Teor. Fiz. **82**, 1562.
L'vov, V.S., and M.I. Shirokov, 1974, Zh. Eksp. & Teor. Fiz. **67**, 1932.
L'vov, V.S., and S.S. Starobinets, 1971, Fiz. Tverd. Tela **13**, 523.
L'vov, V.S., S.L. Moosher and S.S. Starobinets, 1973, Zh. Eksp. & Teor. Fiz. **64**, 1074.
Melkov, G.A., 1971, Zh. Eksp. & Teor. Fiz. **61**, 373.
Melkov, G.A., and I.V. Krutsenko, 1977, Zh. Eksp. & Teor. Fiz. **72**, 564.
Mikhailov, A.S., 1975, Zh. Eksp. & Teor. Fiz. **69**, 523.
Mikhailov, A.S., and A.V. Chubukov, 1984, Zh. Eksp. & Teor. Fiz. **86**, 1401.
Mikhailov, A.S., and R.M. Farzetdinova, 1981, Zh. Eksp. & Teor. Fiz. **80**, 1524.
Mikhailov, A.S., and R.M. Farzetdinova, 1983, Zh. Eksp. & Teor. Fiz. **84**, 190.
Monosov, Ya.A., 1971, Nelineinyi Ferromagnitnyi Rzonans (Nonlinear Ferromagnetic Resonance) (Nauka, Moscow) (in Russian).
Morgenthaler, F.R., 1960, J. Appl. Phys. **31**, 955.
Orel, B.I., and S.S. Starobinets, 1975, Zh. Eksp. & Teor. Fiz. **68**, 317.
Ozhogin, V.I., 1970, Zh. Eksp. & Teor. Fiz. **58**, 2079.
Ozhogin, V.I., and A.Yu. Yakubovsky, 1974, Zh. Eksp. & Teor. Fiz. **67**, 287.
Petrakovksy, G.A., and V.N. Berzhansky, 1970, Zh. Eksp. & Teor. Fiz. Pis'ma **12**, 429.
Plant, J.S., 1977, J. Phys. C **10**, 4805.
Prozorova, L.A., and A.S. Borovik-Romanov, 1969, Zh. Eksp. & Teor. Fiz. Pis'ma **10**, 316.
Prozorova, L.A., and A.I. Smirnov, 1974, Zh. Eksp. & Teor. Fiz. **67**, 1952.
Prozorova, L.A., and A.I. Smirnov, 1975, Zh. Eksp. & Teor. Fiz. **69**, 758.

Prozorova, L.A., and A.I. Smirnov, 1978, Zh. Eksp. & Teor. Fiz. **74**, 1554.
Schlömann, E., 1959, Phys. Rev. **116**, 829.
Schlömann, E., 1962, J. Appl. Phys. **33**, 527.
Schlömann, E., J. Green and V. Milano, 1960, J. Appl. Phys. **31**, 3865.
Seavey, M.H., 1969a, J. Appl. Phys. **46**, 1597.
Seavey, M.H., 1969b, Phys. Rev. Lett. **23**, 132.
Suhl, H., 1957, J. Phys. & Chem. Solids **1**, 209.
Turner, E.M., 1960, Phys. Rev. Lett. **5**, 100.
Turov, E.A., 1959, Zh. Eksp. & Teor. Fiz. **36**, 1254.
Venitsky, V.N., V.V. Eremenko and E.V. Matyushkin, 1978, Zh. Eksp. & Teor. Fiz. Pis'ma **27**, 239.
Waldner, F., D. Barberis and H. Yamazaki, 1984, in: Proc. XXIInd Congress Ampère, eds K.A. Muller et al. (Ampère Comittee, Univ. Zürich) p. 135.
Wang, S., and Ta-Lin Hsu, 1970, Appl. Phys. Lett. **16**, 537.
Wang, S., G. Thomas and Ta-Lin Hsu, 1968, J. Appl. Phys. **39**, 2719.
Woolsey, R.B., and P.M. White, 1969, Phys. Rev. **188**, 813.
Yamazaki, H., 1984, J. Phys. Soc. Jpn. **53**, 1155.
Yamazaki, H., D. Barberis and F. Waldner, 1984, in: Proc. XXIInd Congress Ampère, eds K.A. Muller et al. (Ampère Comittee, Univ. Zürich) p. 123.
Zakharov, V.E., and V.S. L'vov, 1971, Zh. Eksp. & Teor. Fiz. **60**, 2066.
Zakharov, V.E., V.S. L'vov and S.S. Starobinets, 1969, Fiz. Tverd. Tela **11**, 2047.
Zakharov, V.E., V.S. L'vov and S.S. Starobinets, 1970, Zh. Eksp. & Teor. Fiz. **59**, 1200.
Zakharov, V.E., V.S. L'vov and S.L. Moosher, 1972, Fiz. Tverd. Tela **14**, 832.
Zakharov, V.E., V.S. L'vov and S.S. Starobinets, 1974, Usp. Fiz. Nauk **114**, 609.
Zautkin, V.V., and S.S. Starobinets, 1974, Fiz. Tverd. Tela **16**, 678.
Zautkin, V.V., V.S. L'vov, S.L. Moosher and S.S. Starobinets, 1970, Zh. Eksp. & Teor. Fiz. Pis'ma **14**, 310.
Zautkin, V.V., V.S. L'vov and S.S. Starobinets, 1972a, Zh. Eksp. & Teor. Fiz. **63**, 182.
Zautkin, V.V., V.E. Zakharov, V.S. L'vov, S.L. Moosher and S.S. Starobinets, 1972b, Zh. Eksp. & Teor. Fiz. **62**, 1782.
Zautkin, V.V., V.S. L'vov, B.I. Orel and S.S. Starobinets, 1977, Zh. Eksp. & Teor. Fiz. **72**, 272.
Zhotikov, V.G., and N.M. Kreines, 1979, Zh. Eksp. & Teor. Fiz. **77**, 2486.